NAVAL POSTGRADUATE SCHOOL
Monterey, California

THESIS

INVESTIGATION OF AN ARGON-FILLED
THERMOACOUSTIC PRIME MOVER

by

John Dietrick Lamade II

December, 1991

Thesis Advisor Anthony A. Atchley
Co-Advisor D. Felipe Gaitan

Unclassified

SECURITY CLASSIFICATION OF THIS PAGE

REPORT DOCUMENTATION PAGE

Form Approved
OMB No. 0704-0188

1a. REPORT SECURITY CLASSIFICATION Unclassified	1b. RESTRICTIVE MARKINGS
2a. SECURITY CLASSIFICATION AUTHORITY	3. DISTRIBUTION/AVAILABILITY OF REPORT Approved for public release; distribution is unlimited.
2b. DECLASSIFICATION/DOWNGRADING SCHEDULE	
4. PERFORMING ORGANIZATION REPORT NUMBER(S)	5. MONITORING ORGANIZATION REPORT NUMBER(S)
6a. NAME OF PERFORMING ORGANIZATION Naval Postgraduate School 6b. OFFICE SYMBOL (If applicable) 33	7a. NAME OF MONITORING ORGANIZATION Naval Postgraduate School
6c. ADDRESS (City, State, and ZIP Code) Monterey, CA 93943-5000	7b. ADDRESS (City, State, and ZIP Code) Monterey, CA 93943-5000
8a. NAME OF FUNDING/SPONSORING ORGANIZATION 8b. OFFICE SYMBOL (If applicable)	9. PROCUREMENT INSTRUMENT IDENTIFICATION NUMBER
8c. ADDRESS (City, State, and ZIP Code)	10. SOURCE OF FUNDING NUMBERS PROGRAM ELEMENT NO / PROJECT NO / TASK NO / WORK UNIT ACCESSION NO

11. TITLE (Include Security Classification)
INVESTIGATION OF AN ARGON-FILLED THERMOACOUSTIC PRIME MOVER

12. PERSONAL AUTHOR(S)
John Dietrick Lamade II

13a. TYPE OF REPORT	13b. TIME COVERED	14. DATE OF REPORT (Year Month Day)	15. PAGE COUNT
Master's Thesis	FROM _____ TO _____	December 1991	58

16. SUPPLEMENTARY NOTATION
The views expressed in this thesis are those of the author and do not reflect the official policy or position of the Department of Defense or the U.S. Government.

17. COSATI CODES			18. SUBJECT TERMS (Continue on reverse if necessary and identify by block number)
FIELD	GROUP	SUB-GROUP	Acoustics, Thermoacoustics, Prime Mover, Thermoacoustic Heat Transport

19. ABSTRACT (Continue on reverse if necessary and identify by block number)

The goal of this thesis is to investigate the behavior of a thermoacoustic prime mover filled with argon. Data was collected for three different operating conditions: 1) prior to the onset of acoustic oscillation, 2) immediately after onset and 3) after the prime mover had reached steady state, at mean gas pressures of approximately 80 kPa, 205 kPa and 305 kPa. Measured values of 1/Q are compared to predictions of a theory based on Swift's work (Swift, G. W., "Thermoacoustic Engines," J. Acoust. Soc. Am. Vol. 84, October 1988). After onset, Q is determined from measurement of the rise time of the oscillations. The data set collected is the first to span onset and results show good agreement with theory. It is concluded that the theory can be used to provide reasonable input for a model to predict the steady state waveforms.

20. DISTRIBUTION/AVAILABILITY OF ABSTRACT	21. ABSTRACT SECURITY CLASSIFICATION
☒ UNCLASSIFIED/UNLIMITED ☐ SAME AS RPT ☐ DTIC USERS	Unclassified
22a. NAME OF RESPONSIBLE INDIVIDUAL Anthony A. Atchley	22b. TELEPHONE (Include Area Code) (408)646-2848 22c. OFFICE SYMBOL Ph/Ay

DD Form 1473, JUN 86 Previous editions are obsolete

S/N 0102-LF-014-6603

SECURITY CLASSIFICATION OF THIS PAGE
Unclassified

Approved for public release; distribution is unlimited.

Investigation of an Argon-Filled, Thermoacoustic Prime Mover

by

John Dietrick Lamade II
Lieutenant, United States Navy
B.S., United States Naval Academy, 1984

Submitted in partial fulfillment
of the requirements for the degree of

MASTER OF SCIENCE IN PHYSICS

from the

NAVAL POSTGRADUATE SCHOOL
December 1991

ABSTRACT

The goal of this thesis is to investigate the behavior of a thermoacoustic prime mover filled with argon. Data was collected for three different operating conditions: 1) prior to the onset of acoustic oscillation, 2) immediately after onset and 3) after the prime mover had reached steady state, at mean gas pressures of approximately 80 kPa, 205 kPa and 305 kPa. Measured values of 1/Q are compared to predictions of a theory based on Swift's work (Swift, G. W., "Thermoacoustic Engines," J. Acoust. Soc. Am. Vol. 84, October 1988). After onset, Q is determined from measurement of the rise time of the oscillations. The data set collected is the first to span onset and results show good agreement with theory. It is concluded that the theory can be used to provide reasonable input for a model to predict the steady state waveforms.

TABLE OF CONTENTS

I. INTRODUCTION

A thermoacoustic prime mover is a heat engine; it converts stored energy into useful work, in the form of sound. The basic operation and construction of a prime mover can be explained with reference to Fig. 1. For our purposes, a prime mover can be considered to be a closed resonator comprised of five sections. A temperature gradient is applied across the prime mover stack via the ambient and hot heat exchangers. (The terms "ambient" and "hot" refer to the temperatures of the heat exchangers and the portions of the resonator adjacent to them.) The (prime mover) stack and heat exchangers are parallel plates spaced by a few thermal penetration depths and oriented such that the plates lie along the axis of the resonator. The hot and ambient sections are circular tubes -- open at the heat exchanger end and closed at the other end. The net absorption coefficient of the prime mover is the sum of the thermal and viscous wall losses in each of the five sections. Attenuation in the gas is negligible.

As the temperature difference imposed across the stack increases from zero, the thermal losses in the stack decrease and eventually become negative, representing gain. At a sufficiently high temperature difference, the gain of the stack overcomes the remaining losses and the prime mover spontaneously goes into self oscillation. This phenomenon is

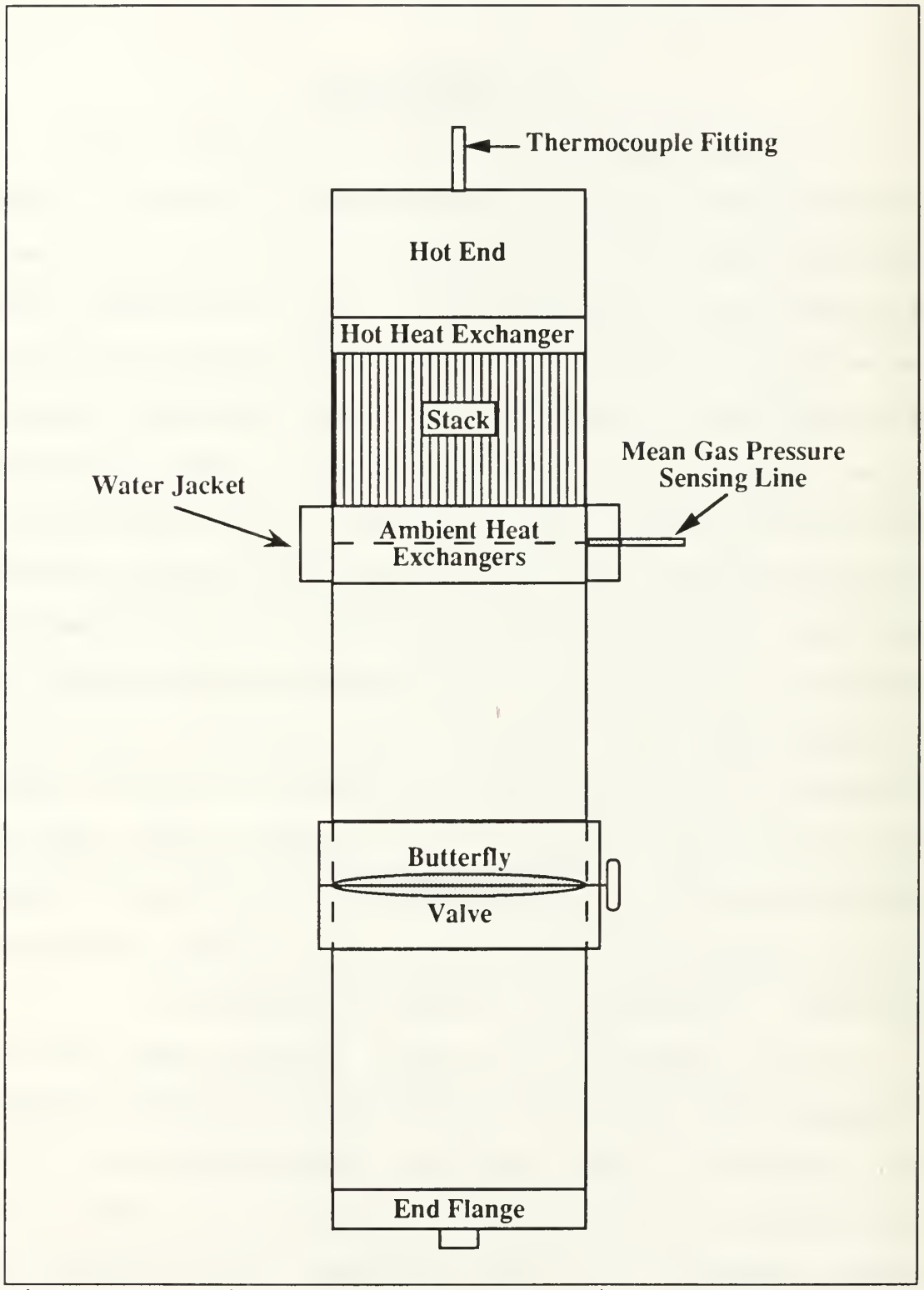

Figure 1. Major components of a prime mover. (Not to scale)

known as onset. Once onset is reached, the acoustic amplitude of the resonator grows rapidly, typically reaching a few percent of the mean pressure. This discussion leads to the conclusion that three distinct regions of prime mover behavior are of interest: 1) below onset, 2) above onset during the buildup of oscillations to steady state, and 3) steady state. The purpose of this thesis is to investigate each of these regions in an argon-filled prime mover.

This thesis is one in a sequence that have investigated thermoacoustic prime movers. The goal of this research is to understand the behavior of prime movers in each of the three regions of operation. In 1989, Lin began a quantitative study of a helium-filled prime mover. He investigated the region below onset as well as documenting the nature of steady state oscillations. Lin found that the steady state oscillations in our prime mover are highly nonlinear, exhibiting a rich harmonic structure. (Lin, 1989) Therefore, it became clear that, to completely understand the steady state region, it is also necessary to understand the generation of harmonics and energy dissipation in high amplitude standing waves. In 1991, Chen began such an investigation in a simple standing wave tube (Chen, 1991). Also in 1991, Bowers investigated the initial buildup of oscillations above onset (Bowers, 1991).

As stated earlier, the purpose of this thesis is to investigate the three regions of behavior in an argon-filled prime mover. One reason for this is to add to our

understanding of prime movers by using a gas other than helium. Also, Lin and Bowers used slightly different prime movers so direct comparison of their data is not possible. We will use the same prime mover configuration below and above onset so that we can have a complete data set from zero temperature difference through onset and beyond.

Following a discussion of applicable theory, the experimental setup and procedures used to collect data will be presented. The results and their analysis follow, along with a discussion of sources of error. Finally, a summary of this experiment and its conclusions will be made along with recommendations for subsequent research in this area.

II. THEORY

Theoretically, the performance of a prime mover can be investigated through the calculation of its acoustic power output. However, below onset and during the initial buildup of oscillations, it is easier to measure the quality factor of the prime mover.

The net acoustic power output, $\dot{W}$, can be related to the quality factor, Q. Below onset, Q is easily determined from the prime mover's frequency response. Just above onset, Q can be determined from the rise time of the oscillations. This section contains a discussion of the theory necessary to calculate 1/Q in both regions. This discussion is a summary of that found in Bowers (Bowers, 1991, pp. 10-15) which draws heavily from Swift (Swift, 1988).

The reciprocal of the quality factor, 1/Q, of the prime mover can be expressed as

$$\frac{1}{Q} = \frac{-\dot{W}}{\omega E_{ST}} \qquad (1)$$

where ω is the angular frequency and E_{ST}, the stored energy of the resonant tube. $\dot{W}$ is determined by integrating the power per unit volume, $\dot{w}(x)$, over the volume of the prime mover, as follows,

$$\dot{W} = \int_{x=0}^{L} \dot{w}(x)\, S(x)\, dx \ . \tag{2}$$

S(x) is the cross-sectional area of the prime mover at x.

In the stack, $\dot{w}(x)$ is

$$\dot{w}(x) = \frac{1}{2} Re \left[\frac{P_A^2 \omega}{\rho_m a^2} \left\{ j \left(\frac{\tilde{f}_\kappa - \tilde{f}_\nu}{1 - \tilde{f}_\nu} \frac{1 + \frac{1}{y_o}}{(1-\sigma)(1+\epsilon_s)} \frac{\nabla T_m}{k T_m} \tan(kx) \right.\right.\right. \tag{3}$$

$$\left.\left.\left. + 1 + \frac{\gamma - 1}{1+\epsilon_s} \tilde{f}_\kappa \right) \cos^2(kx) - j \frac{\left(1 + \frac{1}{y_o}\right)^2}{1 - f_\nu} \sin^2(kx) \right\} \right].$$

P_A and k are the peak pressure amplitude and wave number of the standing wave, whereas a and σ represent the thermodynamic sound speed and Prandtl number of the working fluid. $j^2 = -1$. Also, ∇T_m is the mean temperature gradient along the stack plates and T_m is the mean temperature of the plate and is a function of x. $\tilde{f}_\nu$ is defined as

$$\tilde{f}_\nu = \frac{\tanh\left[\frac{(1+j)y_o}{\delta_\nu}\right]}{(1+j)\frac{y_o}{\delta_\nu}} \tag{4}$$

for parallel plates. δ_ν, the viscous penetration depth, is defined as

$$\delta_\nu = \sqrt{\frac{2\mu}{\rho_m \omega}} \ . \tag{5}$$

μ is the fluid's dynamic viscosity. A similar relationship exists between $\bar{f}_\kappa$, δ_κ and y_o, although δ_κ is defined as

$$\delta_\kappa = \sqrt{\frac{2K}{\rho_m c_p \omega}} \quad . \tag{6}$$

K is the thermal conductivity of the working fluid.

ϵ_s defines the relative heat capacity of the gas compared to the plates

$$\epsilon_s = \frac{\rho_m c_p \delta_\kappa \tanh\left[\frac{(1+j)y_o}{\delta_\kappa}\right]}{\rho_s c_s \delta_s \tanh\left[\frac{(1+j)l}{\delta_s}\right]} . \tag{7}$$

where ρ_m and c_p are the mean density and isobaric specific heat of the working fluid and ρ_s, c_s and δ_s represent similar qualities for the stack plates. l is one-half the stack plate thickness. In the heat exchangers, $\dot{w}(x)$ is identical to Equation (3), except $\Delta T_m = 0$. In the ambient and hot ends, $\dot{w}(x)$ is given by Equation (3) with $\Delta T_m = 0$ and $l = 0$ (there are no plates). Also, the functions $\bar{f}_\nu$ and $\bar{f}_\kappa$ take on different forms involving the Bessel functions.

E_{ST} is determined by integrating the time averaged energy density over each prime mover section,

$$E_{ST} = \frac{1}{4}\frac{P_A^2 S}{\rho_m a^2}\Bigg[x_{amb\ end} + \int_{amb\ hx}\left[\frac{\cos^2(kx+\phi)}{1+\frac{1}{y_o}} + \left(1+\frac{1}{y_o}\sin^2(kx+\phi)\right)\right]dx + \int_{stack}\left[\frac{\cos^2(kx+\phi)}{1+\frac{1}{y_o}} + \left(1+\frac{1}{y_o}\sin^2(kx+\phi)\right)\right]dx + \int_{amb\ hx}\left[\frac{\cos^2(kx+\phi)}{1+\frac{1}{y_o}} + \left(1+\frac{1}{y_o}\sin^2(kx+\phi)\right)\right]dx + x_{hot\ end}\Bigg] . \quad (8)$$

where S is the cross-sectional area of the resonator and ϕ is the phase of the standing wave as it enters each section.

These equations use the properties of the working fluid and the initial conditions of the prime mover to predict 1/Q as a function of ∇T_m across the stack.

The resonance frequency is calculated by neglecting the dependence of the sound speed, *a*, on dissipation. In other words *a* is assumed to be the thermodynamic sound speed. Next, we require that acoustic pressure antinodes exist at each end of the prime mover which amounts to requiring that

$$\int_0^L k(x)\,dx = n\pi . \tag{9}$$

k depends on x through $k(T_m(x))$.

III. EXPERIMENT

A. EXPERIMENTAL SETUP

The prime mover and temperature and pressure monitoring/control systems are same ones used in Bowers' thesis. Only pertinent details will be given here.

1. The Prime Mover

As discussed earlier and shown in Fig. 1, the prime mover is composed of five sections.

a. The Hot End

The hot end of the prime mover consists of a nickel tube, 0.63 cm thick, 5.5 cm long and having an inner diameter of 3.82 cm. A nickel cap is welded into the top of this tube to provide a rigid boundary. To monitor the hot end temperature, a small hole is drilled into the end cap and fitted with an access tube for a K-type thermocouple. The lower end of this assembly holds the hot heat exchanger.

b. The Hot Heat Exchanger

The hot heat exchanger is also composed of nickel and like the hot end, has an inner diameter of 3.82 cm. 25 nickel plates, 0.045 cm thick and 0.762 cm long are mounted along the heat exchanger's longitudinal axis. The spacing between these plates is 0.104 cm. 304 stainless steel spacers mounted to one side of each plate help maintain this spacing

and prevent deformation under high heat conditions. The hot end/heat exchanger assembly is welded to the prime mover stack.

c. The Prime Mover Stack

The prime mover stack is housed in a thin walled 304 stainless steel tube, 3.5 cm long, with an inner diameter of 3.82 cm and a wall thickness of 0.05 cm. The stack consists of 35, 304 stainless steel plates, 0.028 cm thick, spaced 0.077 cm apart. As in the hot heat exchanger, the spacing between these plates is maintained by using 304 stainless steel spacers mounted to one side of each plate.

d. The Ambient Heat Exchanger

A constant ambient temperature is maintained at the bottom of the stack by using 2 identical copper heat exchangers. Each is 1.02 cm long and consists of 25 copper plates, 0.025 cm thick and spaced 0.105 cm apart. The inner diameter of each heat exchanger is 3.82 cm. The two heat exchangers are spaced 0.15 cm apart. The top heat exchanger is mounted in contact with the lower end of the prime mover and positioned so that its plates form right angles with the stack plates. This maximizes fluid flow out of the stack by ensuring that the heat exchanger plates do not block the gaps between the prime mover plates. The second heat exchanger is not necessary for the purposes of this thesis. It will be used in later investigations.

A constant working temperature is maintained within the heat exchangers by mounting them in a brass water jacket. This water jacket also contains a small hole used for pressurizing the prime mover. The hot end heat exchanger/stack assembly is soldered to the top of the water jacket.

e. The Ambient End

The ambient end of the prime mover consists of a 3.82 cm ID, 88.11 cm long copper tube, flanged at the bottom to accommodate an end cap. Two different end caps are used. Below onset the end cap houses an electret driver and an electret microphone, so that the frequency response of the tube can be determined. The end cap used to collect data after onset holds only a microphone to record the amplitude of the standing wave.

A butterfly valve is located 38.0 cm from the bottom of the ambient heat exchanger. Closing the butterfly valve effectively shortens the length of the prime mover and requires a greater differential temperature to drive the prime mover to onset. With the butterfly valve closed, a differential temperature across the stack sufficient for onset can be established without actually generating a standing wave (Bowers, 1991, p. 18).

2. Control and Monitoring Systems

a. Temperature

The hot end of the prime mover is fitted with an Omega Engineering HBA Model 202040 heater. Power is supplied to the heater by a General Radio Type 100-Q variable transformer which controls the heater voltage. The heater coils are wrapped tightly around the hot end of the prime mover and stainless steel shim stock is used to maintain good thermal contact. A Neslab RTE-110 constant temperature bath supplies cooling water to the water jacket and to plastic tubing which encircles the entire length of the ambient end of the prime mover.

Temperatures along the length of the prime mover are monitored by a Keithley Model 740 System Scanning Thermometer. A K-type thermocouple probe is inserted into the access hole in the hot end until that it makes contact with the hot heat exchanger. Three E-type thermocouple junctions are affixed to the outside of the ambient end of the prime mover with cyanoacrylate adhesive. These junctions are placed below the ambient heat exchanger, below the butterfly valve and above the pressure transducer flange at the bottom of the ambient end.

b. Pressure

The prime mover in this thesis uses argon gas as the working fluid. The gas pressure is controlled by a Matheson 8H-580 pressure regulator with a working range of 0 - 1400 kPa. Prior to pressurization, the prime mover is evacuated using a Welch Model 1400 Duo-Seal Vacuum Pump for several hours to ensure all residual gases are removed. Pressure within the prime mover is monitored via the pressure sensing line in the waterjacket assembly. An external tubing and valve network allows the pressure sensing line to be isolated from the gas supply cylinder and vacuum pump. The pressure is monitored by an Omega PX304-300AV pressure transducer having a sensitivity of 3PSIA/MVDC. The output of the pressure transducer is read by a Hewlett Packard 3457A digital multimeter.

B. EXPERIMENTAL PROCEDURE

As power is supplied to the hot end of the prime mover, the differential temperature, ΔT_m, increases from zero to a level sufficient to bring about onset. Data was acquired in the three regions of prime mover operation discussed in the Introduction.

1. Below Onset

a. Data Acquisition

A schematic diagram of the apparatus used to measure frequency response of the prime mover below onset is

shown in Fig. 2. Data acquisition is controlled using GPIB hardware and a program written in Microsoft QuickBasic and executed on a Standard 286 PC-AT. After entering the expected resonance frequency, desired bandwidth, number of frequency increments and starting system pressure, the PC directs a Hewlett-Packard 3324A Synthesized Frequency Generator to output a 10 Vpp sine wave beginning at the lower end of the desired bandwidth. This signal is sent to the reference input of a Stanford Research Systems 530 Lock-In Amplifier, a Kikusui COS6100A Oscilloscope and a Techron 7520 Power Supply Amplifier which amplifies the signal and sends it to the driver.

The driver is a locally constructed electret type which sets up a standing wave in the prime mover. An electret microphone is used to sense the amplitude of the standing wave. The output of the microphone is first directed through a locally constructed preamplifier which boosts the signal by a factor of 100. The amplified signal is then sent to the lock-in amplifier and oscilloscope.

The oscilloscope provides a visual display of the reference signal and the received signal, while the lock-in amplifier filters the received signal in a narrow bandwidth around the reference frequency. It sends the in-phase and quadrature components of the signal to the HP 3457A multimeter. These values are read by the PC, via a GPIB interface, and the amplitude of the signal is determined.

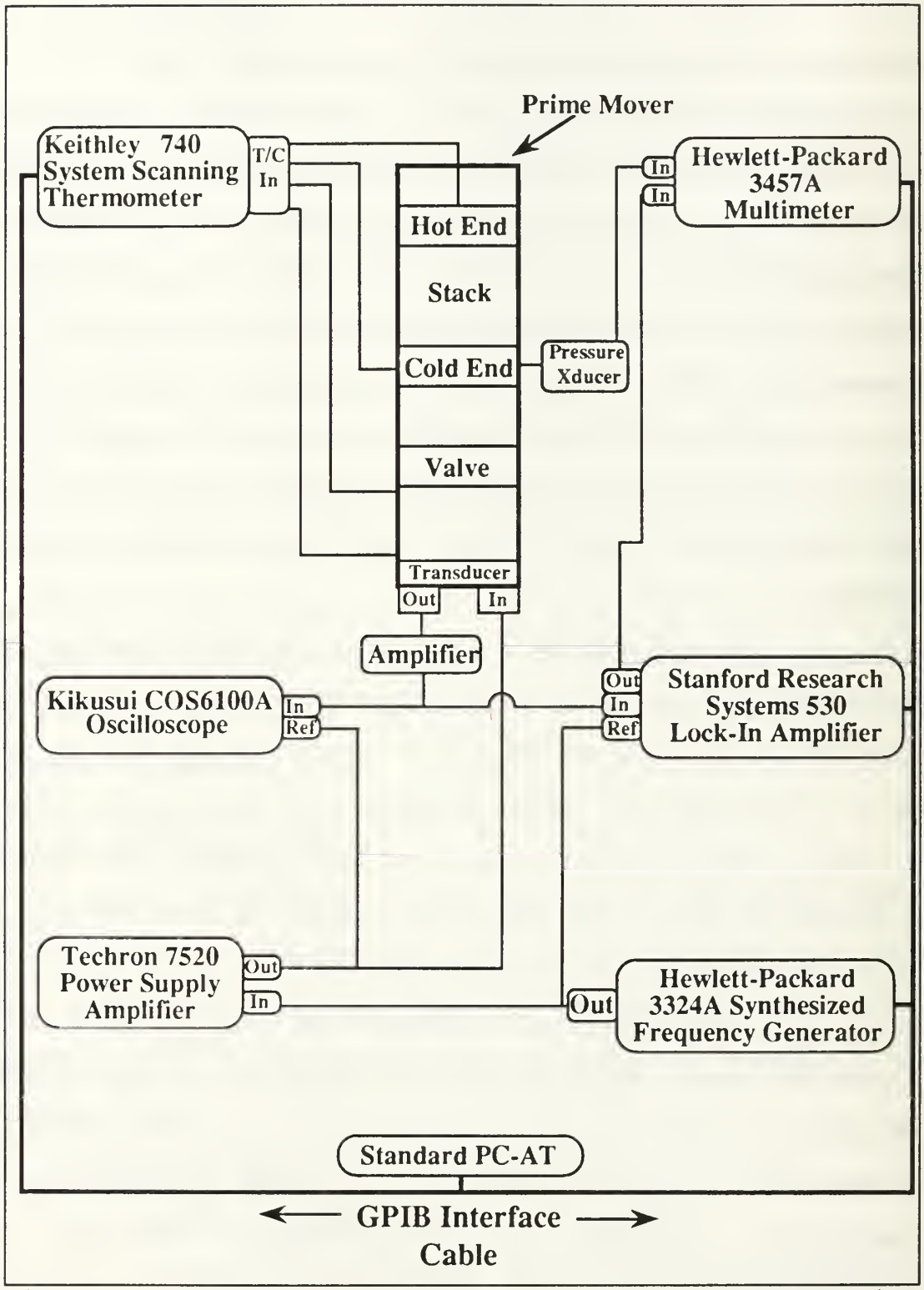

Figure 2. Diagram of Apparatus Used to Collect Data Prior to Onset

After the acoustic amplitude data and the temperature of each thermocouple are written to a worksheet, as shown in Fig. 3, the frequency is incremented. This procedure is repeated until the end of the bandwidth is reached, at which time the ending system pressure is recorded. Data was recorded for both the fundamental and second modes of the prime mover at the three mean gas pressures of interest.

b. Data Processing

Q is obtained by applying the same fitting function Lin used to determine the resonant response of a simple tube. That function is

$$P = A\left(\frac{f}{f_o}\right)^2\left|\frac{\cot(kL)}{kL}\right|, \tag{9}$$

where P is the normalized amplitude of the acoustic pressure in the tube and A is a scaling constant. The subscript "o" indicates a measured resonant value. kL is defined as

$$kL = \pi\left[\frac{w}{w_o} + \frac{j}{(2Q)}\right]. \tag{10}$$

By performing a least squares fit of P versus f, values for f_o, A and Q can be determined. (Lin, 1989, p. 22) Data is processed using macro routines in Microsoft's Excel program. Figure 4 shows a typical plot resulting from the fitting procedure.

	A	B	C	D	E	F	G
1	File Name: 31030011.XLS						
2	Gas Type: Argon						
3	Microphone Gain: 100						
4	F. Gen. Amplitude: 10000mV						
5	Center Frequency : 161 Hz						
6	Start Pressure: 306.7159 KPa						
7							
8	fo	A	Q				
9	161.26	0.99483	147.76				
10							
11	Freq(Hz)	Amplk(mV)	Phase(rad)	T02(DegC)	T03(DegC)	T04(DegC)	T05(DegC)
12	160.0006	10.72061	0.391125	308.9	20.6	20.4	20.4
13	160.2008	13.37106	0.365257	308.9	20.6	20.4	20.4
14	160.4005	15.48943	0.434295	308.9	20.6	20.4	20.4
15	160.6005	19.19547	0.565027	308.9	20.6	20.4	20.4
16	160.8008	23.49876	0.827011	308.9	20.6	20.4	20.4
17	161.0009	27.43512	1.046905	308.9	20.6	20.4	20.4
18	161.2008	29.3778	1.366104	308.9	20.6	20.4	20.4
19	161.4003	27.86031	1.690933	308.9	20.6	20.4	20.4
20	161.6009	25.73375	1.989192	308.9	20.6	20.4	20.4
21	161.8006	22.04756	2.247514	308.7	20.6	20.4	20.4
22	162.0009	17.27475	2.421878	308.6	20.6	20.4	20.4
23							
24	End Pressure: 297.1531 KPa						
25	Average Pressure: 301.9345 KPa						
26							
27	P avg	T top	S dev	T bott	S dev	Fo	Q
28	301.9345	308.8364	0.102691	20.6	4.26E-07	161.26	147.76

Figure 3. Sample worksheet used to record data prior to onset.

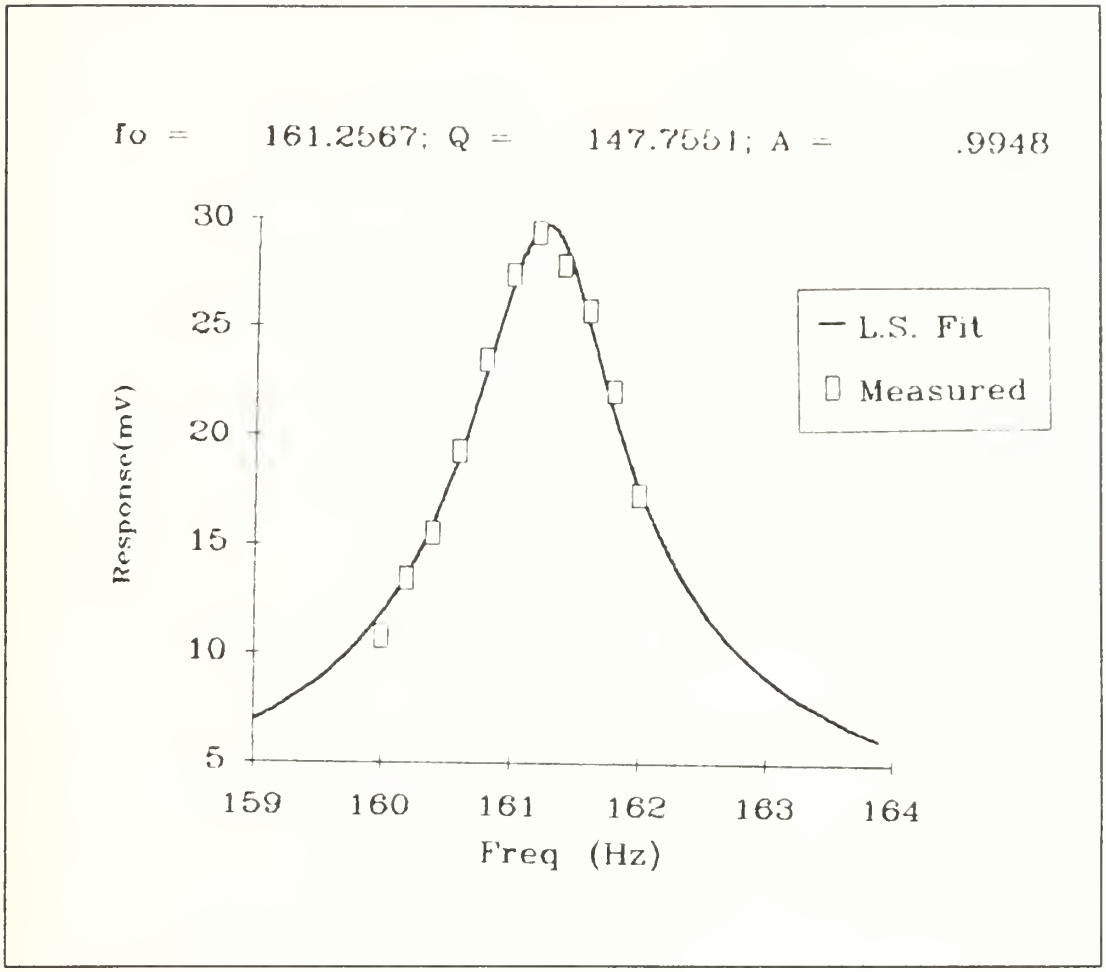

Figure 4. Sample plot of data obtained prior to onset.

To compensate for any loss of pressure during the run, the mean gas pressure is obtained by averaging the starting and ending system pressures. The mean hot and ambient end temperatures are the averages of the temperatures recorded at each incremental frequency.

2. Determining Onset

Unlike helium, which exhibits a well-defined onset temperature when used as the working fluid, it was more

difficult to identify the experimental onset temperature in argon.

As onset was approached, a very low amplitude acoustic wave was detected by the sensing equipment. The amplitude of this wave increased slowly, requiring, in some cases, several minutes to build to steady state. The exact reason for this behavior is unknown. The temperature differences required for onset are shown in Table 1. These values were determined by slowly increasing ΔT_m until onset occurred, then observing the behavior of the prime mover at several temperatures around this reference point. ΔT_{Onset} is the mean value of the temperatures for which onset was observed. At onset, $1/Q = 0$.

Pressure (kPa)	80	205	305
ΔT_{Onset} (°C)	366.4	381.7	403.5

Table 1. SUMMARY OF ONSET TEMPERATURES

3. Above Onset

a. Data Acquisition

A schematic diagram of the apparatus used to collect data above onset is shown in Fig. 5. The pressure transducer used for this phase of data collection is an ENDEVCO Model 8510B-5 piezoresistive microphone with a linear response range of ± 5 PSI. Data is collected above onset using the procedures outlined in Bowers' thesis. With the

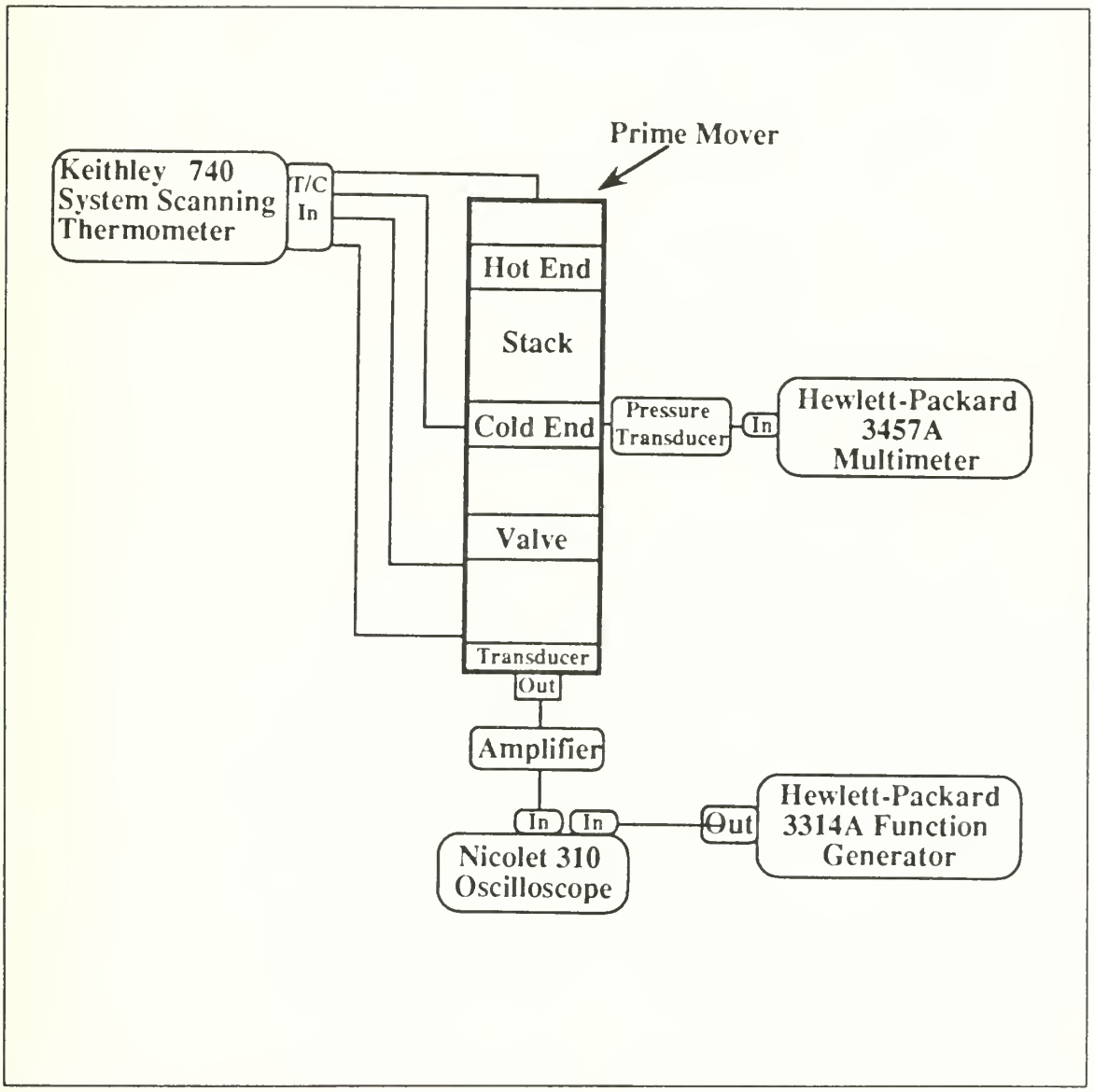

Figure 5. Diagram of apparatus used to collect data after onset.

is established and allowed to stabilize. When the butterfly valve is opened, acoustic oscillations begin to build up in the prime mover. The resulting acoustic wave is sensed by the microphone and routed through a locally constructed, differential amplifier having a gain of 10. This signal is sent to a Nicolet 310 digital oscilloscope for recording and storage. (Bowers, 1991, p 20) The oscilloscope is triggered to begin recording data immediately after onset occurs, ensuring that the acoustic signal is small. This minimizes the presence of harmonics in the recorded signal and ensures that the temperature distribution in the stack is unaltered by significant acoustic heat transport.

b. Data Processing

The Q of the prime mover above onset is determined by the relationship,

$$Q = \frac{\omega}{2\beta}, \tag{11}$$

where ω is the angular resonance frequency and β is the temporal absorption coefficient. To ascertain the value of these variables, the data collected above onset is digitally processed using the techniques developed by Bowers (Bowers, 1991, pp 22-27).

The binary signal stored by the Nicolet 310 is converted to ASCII code to be processed using Mathworks MATLAB program. Initially, a discrete Fourier transform, DFT, is

performed and the positions of the resonance frequency and any harmonics are determined. A raw waveform is shown in Fig. 6, while Fig. 7 shows the DFT of this data.

The original signal is multiplied by a complex exponential term which effectively shifts the fundamental frequency to DC (i.e. 0 Hz). A 5th order, 50 Hz Butterworth filter is then applied to the shifted data set to isolate the fundamental frequency. Figure 8 shows a plot of the shifted, filtered data revealing that only the envelope of the original data remains. As shown in Bowers' thesis, the end effects of the Butterworth filter can be avoided by disregarding the first 300 and last 300 points of filtered data. The exponential envelope of the original waveform is linearized by taking the logarithm of the normalized amplitude, so that aleast mean squares fit can be performed. The slope determined by this fit corresponds to the desired quantity, β.

4. Steady State

a. Data Acquisition

Collection of data once the prime mover has reached steady state uses the same experimental setup as was used to collect data above onset. With the butterfly valve open and a sufficient ΔT_m established to induce self oscillation, the prime mover is allowed to reach equilibrium and the resulting waveform is recorded by the Nicolet oscilloscope.

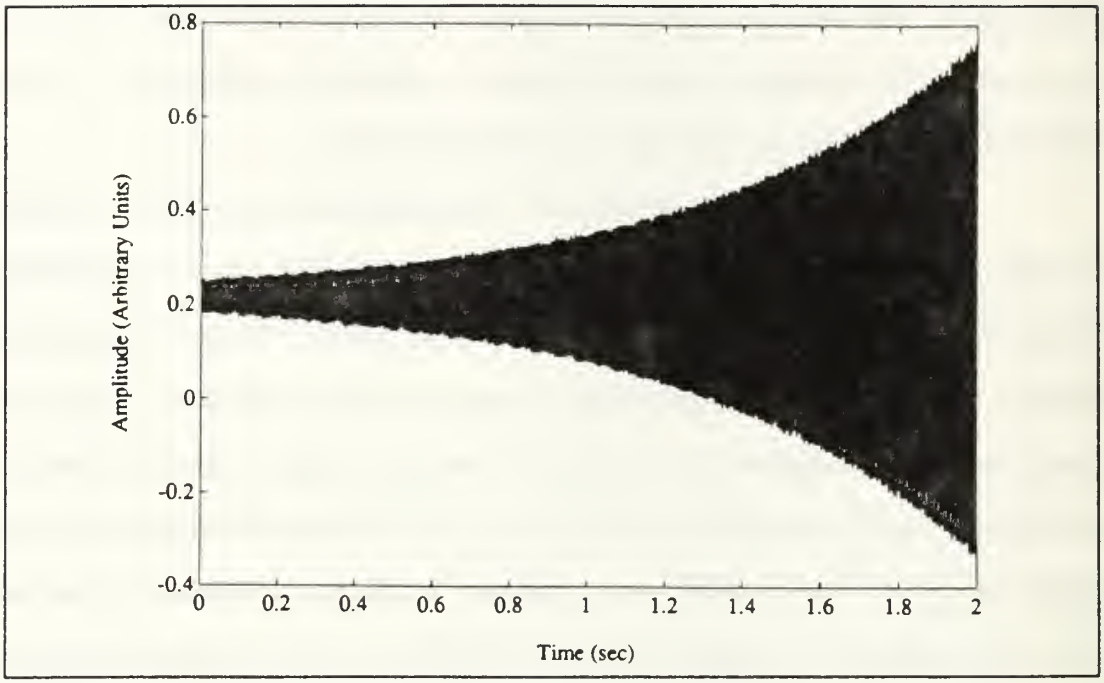

Figure 6. Sample plot of data collected during onset.

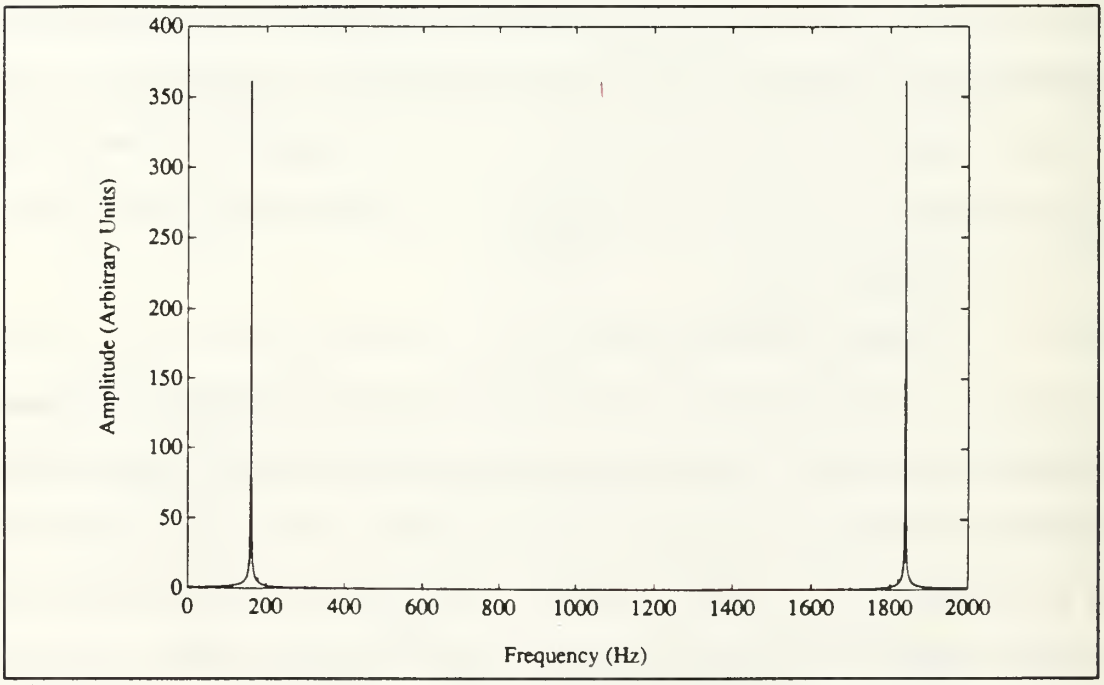

Figure 7. Plot of DFT of data collected during onset.

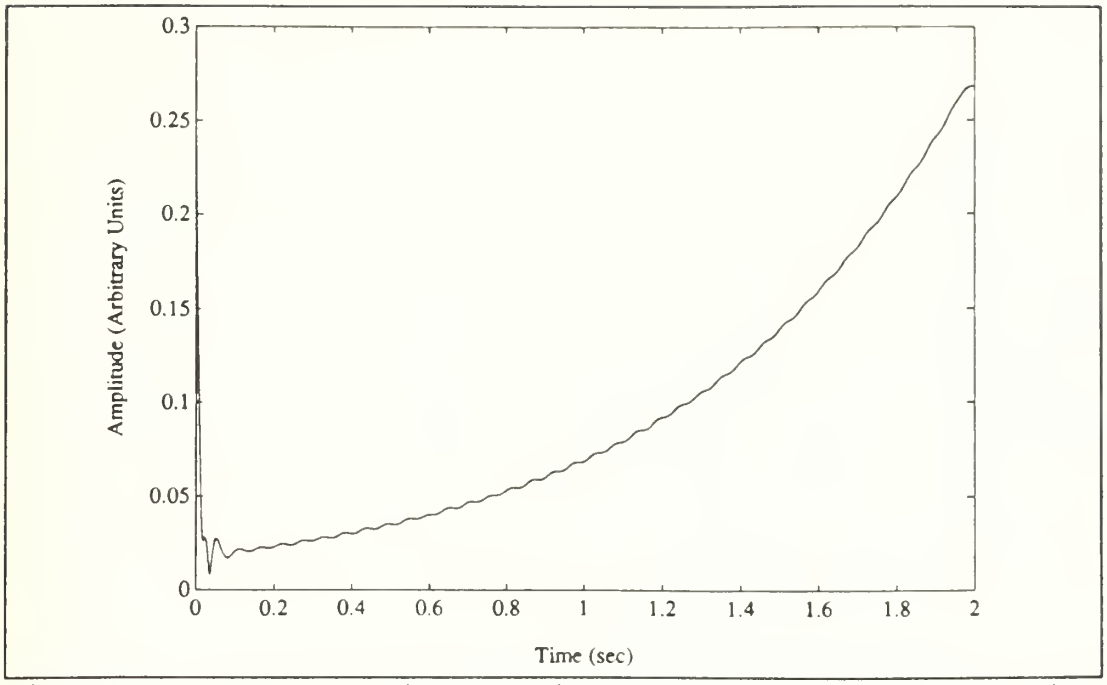

Figure 8. Plot of shifted, filtered data collected during onset.

In order to prevent aliasing, the digital sampling rate must conform to the Nyquist criteria,

$$f_{Nyquist} \geq 2 f_{max}, \qquad \textbf{(12)}$$

where $f_{Nyquist}$ is the minimum sampling frequency and f_{max} is the highest frequency of interest in the signal being sampled. (Strumm, 1988, p 54) Since the fundamental frequency of the prime mover is approximately 160 Hz and there will be at most 10 harmonics detectable in the steady state, f_{max} = 1760 Hz and $f_{Nyquist}$ = 3520 Hz. This corresponds to a minimum sampling rate of 308 μs per point. We used 200 μs per point.

Since we are interested in the absolute pressure amplitude of the harmonics of the steady state waveform, a known test signal is also recorded, using the same oscilloscope settings. The DFT of this signal will provide a reference when analyzing the original data.

b. Data Processing

Using Mathworks MATLAB program, a DFT of the reference signal and the recorded waveform are performed, as shown in Figs 9 and 10. In the interest of clarity, Fig. 9 shows only the first 1000 points of the original signal's 4000 point DFT, while only the first half of the DFT of the recorded waveform is shown in Fig. 10.

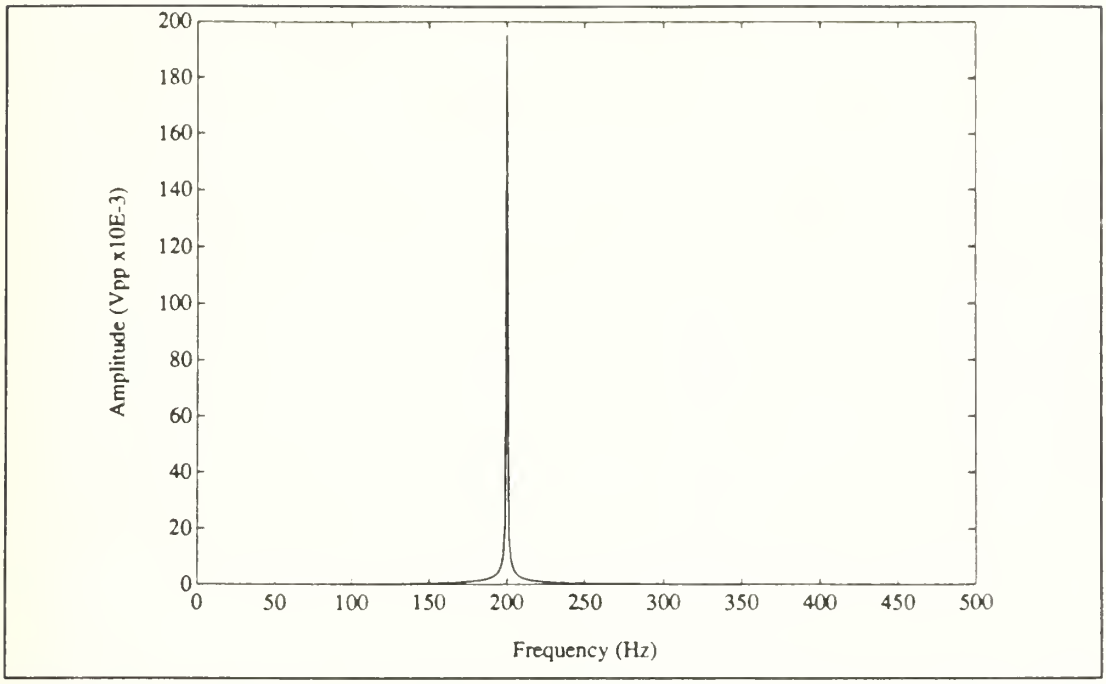

Figure 9. Plot of DFT of reference signal used for analysis of steady state data.

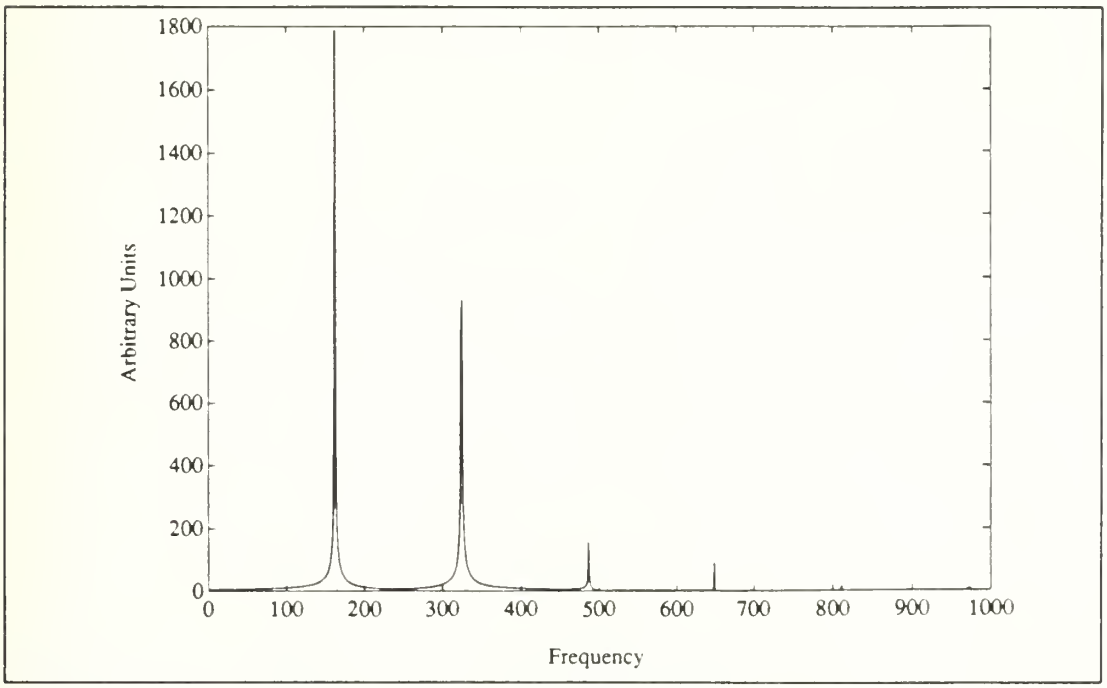

Figure 10. Sample plot of DFT of data collected during steady state.

IV. RESULTS

Data were taken at 80 kPa, 205 kPa and 305 kPa for ΔT_m 's ranging from 0°C to approximately 425°C, the self-imposed safe working limit for the prime mover assembly. Below onset, data for the fundamental and second modes were collected at all three pressures. However, due to temperature constraints, only the two lower pressures were investigated above onset and at steady state.

1. Results of 1/Q Measurements

Figures 11 and 12 show the combined results of the data collected below onset and immediately above onset for pressures of 80 kPa and 205 kPa. Fig. 13 shows the results obtained below onset at 305 kPa. For discussion purposes, it should be pointed out that 1/Q is proportional to the net attenuation in the prime mover.

The first point of discussion is that the data in Figs. 11 and 12 show a smooth transition from below onset, up to and beyond onset. This feature indicates that the methods of determining 1/Q in each region are consistent. These data are the first to show the progression from below onset to above onset. It should be pointed out that the above onset data were obtained at low acoustic amplitudes. This ensures

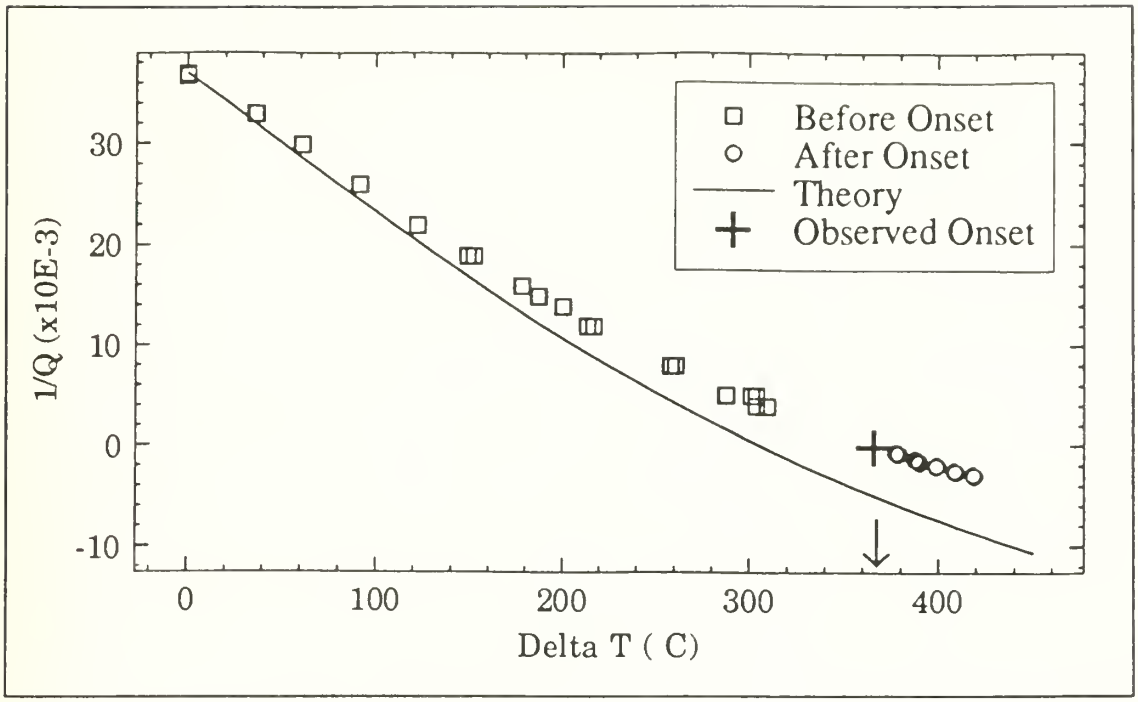

Figure 11. Plot of combined 1/Q vs ΔT_m data obtained below and immediately after onset. P = 80kPa.

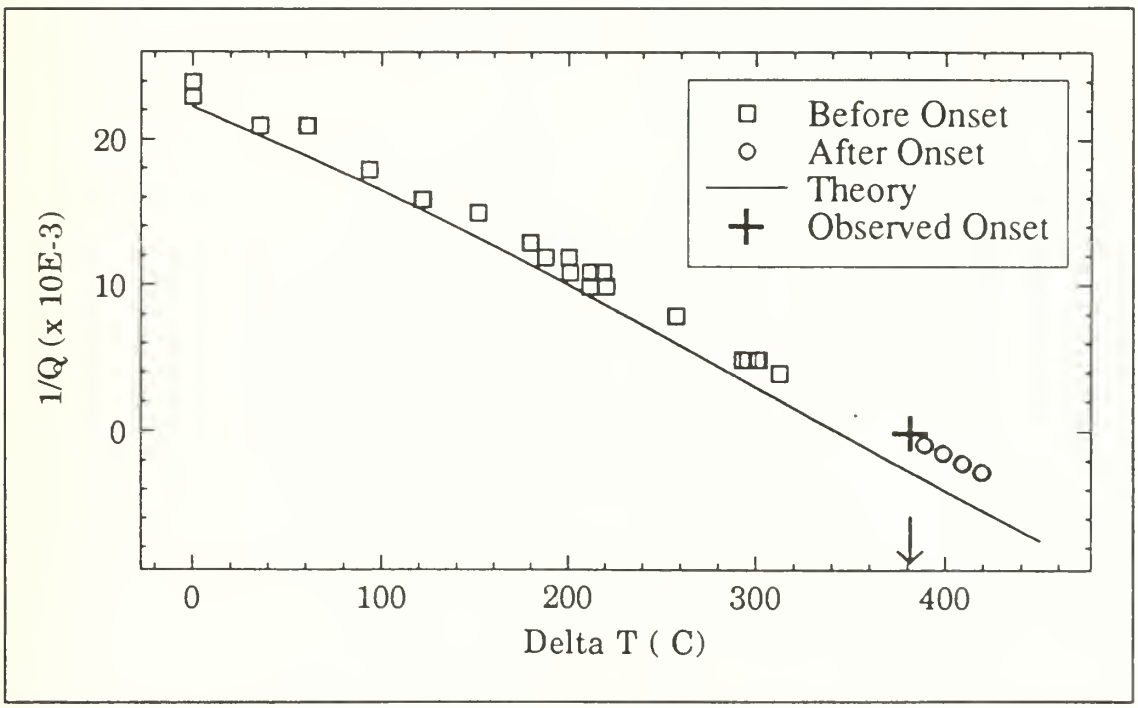

Figure 12. Plot of combined 1/Q vs ΔT_m data obtained below oand immediately after onset. P = 205 kPa.

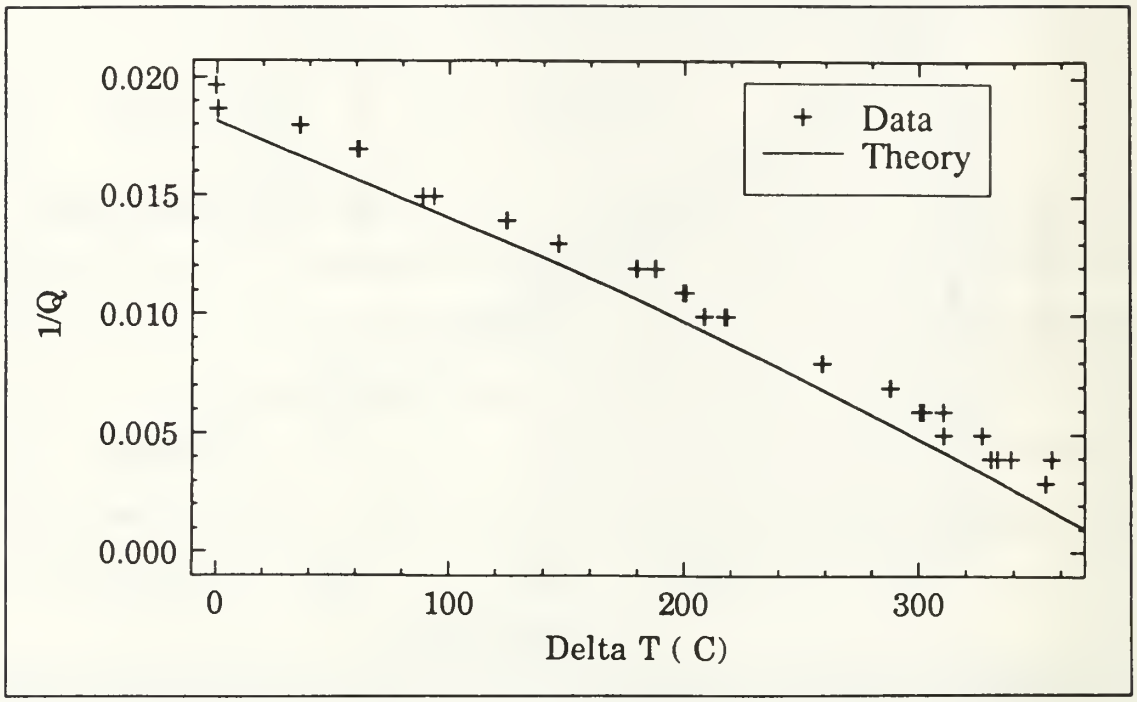

Figure 13. Plot of 1/Q vs ΔT_m for data obtained below onset in the fundamental mode. P = 305 kPa.

that the effects of acoustic heat transport can be ignored, just as they were below onset. The results for the second mode are shown in Figs. 14, 15 and 16. All of these data were obtained below onset.

The agreement between data and theory is good, however, there is a tendency to underpredict the attenuation. This trend is especially evident in the second mode. One possible explanation for this is the fact that the model does not include the presence of the butterfly valve. The magnitude of this effect should be roughly proportional to the additional surface area introduced by the valve. The valve is a circular disk of negligible thickness with a diameter of

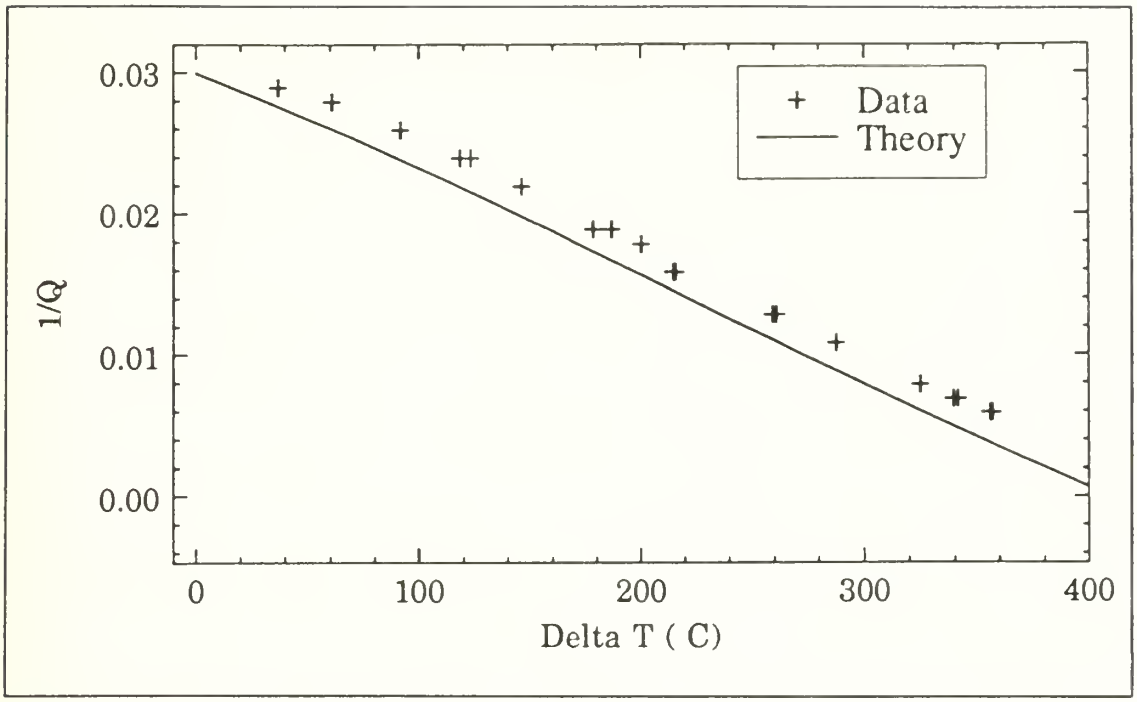

Figure 14. Plot of 1/Q vs ΔT_m for data obtained below onset in the second mode. P = 80 kPa.

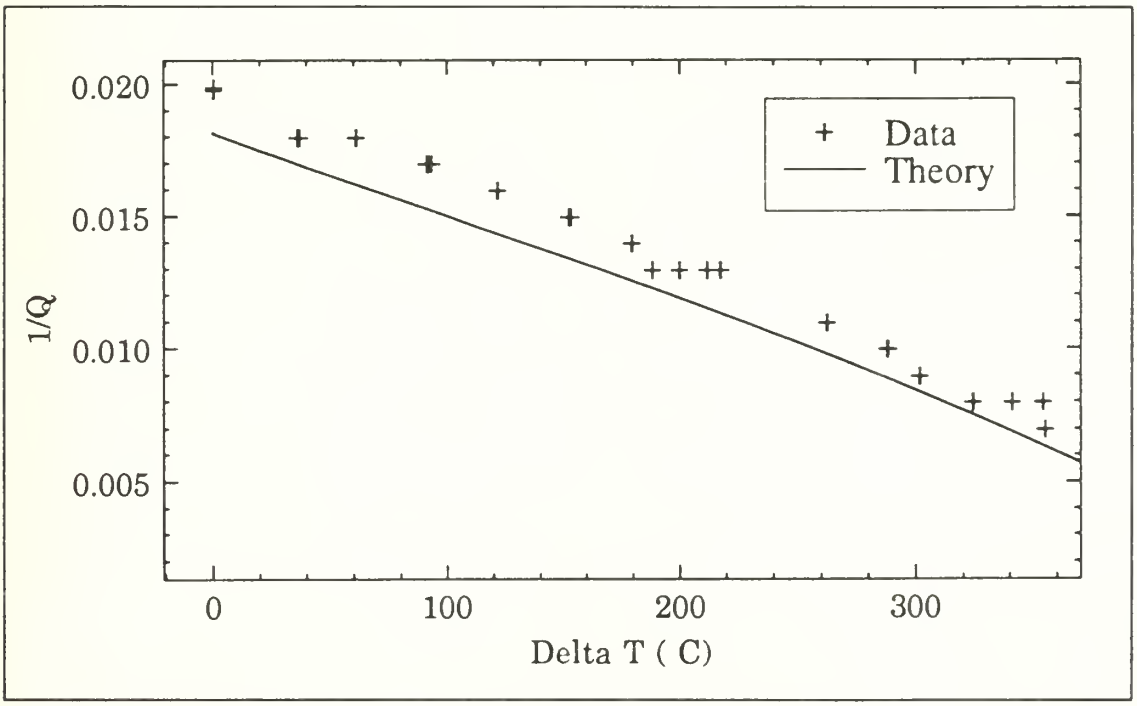

Figure 15. Plot of 1/Q vs ΔT_m for data obtained below onset in the second mode. P = 205 kPa.

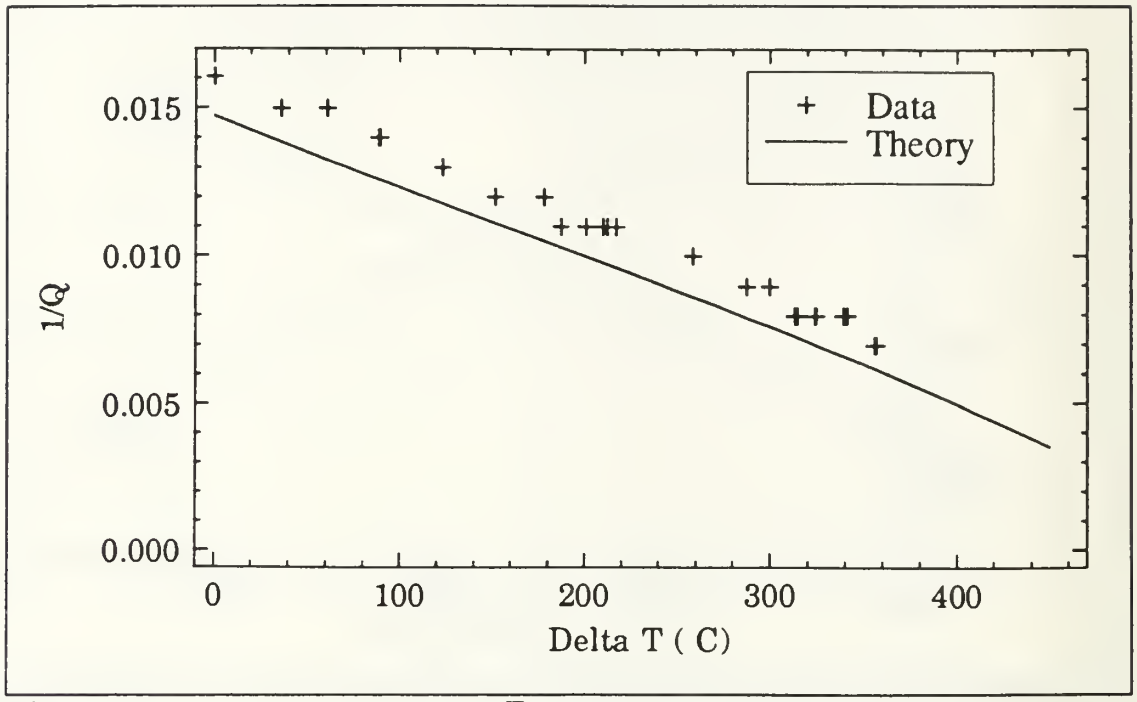

Figure 16. Plot of 1/Q vs ∇T_m for data obtained below onset in the second mode. P = 305 kPa.

approximately 38 cm. The total surface area is, therefore, approximately 24 cm^2. The total surface area of the primemover, including heat exchangers and prime mover stack, is approximately 2300 cm^2. Therefore, the valve adds approximately 1 percent more surface area to the prime mover. Although a more detailed calculation of the effect of the valve is needed, it is unlikely that it alone can account for all the error. It should be pointed out that the same trend is evident in helium data. (Atchley, 1991)

Another possible explanation concerns the fact that T_{hot} and T_{cold} are recorded at the top of the hot heat exchanger

and the bottom of the ambient heat exchanger, respectively. These temperatures may not accurately reflect the actual temperature difference across the stack. This suggests that the actual ΔT_m is less than that measured, an error that would in effect shift the data to the left, providing a much better overall agreement. The magnitude of this error is difficult to measure. Measurements performed to try and estimate the error revealed that the results were very sensitive to the degree of contact between the heat exchangers and the stack. A discrepancy of $\pm$ 10°C is certainly not unreasonable. However, without knowing the degree of contact in the prime mover, any estimates of the magnitude of the error are speculation.

Another point of comparison has to do with the dependence of the difference between theory and experiment on ΔT_m. Figures 11 and 12, and, to a lesser extent, Fig. 13, show that the agreement is worse at higher values of ΔT_m. This trend is absent in Figs. 14, 15 and 16. A possible explanation for this trend may the irregularities in stack geometry. The theory assumes plate spacing is uniform, however, this is not the case. One would expect this effect to be most pronounced when δ_κ is comparable to y_o. Recalling the definition of δ_κ from Eqn. (6), this would be true for low pressures and frequencies. This follows exactly the trend noted.

2. Other Sources of Error

In addition to the specific sources of error previously mentioned, there are others associated with the apparatus and procedures which apply to all data collected.

a. Monitoring Systems

The measurements of mean gas pressure, P_m, and system temperatures are subject to instrumentation errors and errors due to averaging. T_c and T_h are used to determine ΔT_m, while T_c and P_m are inputs to the equation used for theoretical prediction of prime mover response.

For example, when investigating the response of the fundamental mode at $P_m \approx 205$ kPa and $\Delta T_m \approx 150^{\circ}C$, the average value of T_h over the course of data collection is $172.2 \pm 0.5\ ^{\circ}C$ and $T_c = 20.2 \pm 0.03\ ^{\circ}C$ As a result $\Delta T_m = 152.0 \pm 0.5\ ^{\circ}C$, an error of 0.33 percent. P_m is the average of the mean system pressures at the start and finish of each data collection run. Actual system pressure varies over the course of collecting data due to small leaks in the prime mover. Typically, the system lost one percent of pressure at 205 kPa, two percent at 305 kPa and gained 0.2 percent at 75 kPa.

The prediction of prime mover behavior for a given pressure and mode requires T_c and P_m as input. These parameters are obtained by averaging their values for an entire data set. For example, in the fundamental mode at

approximately 205 kPa, T_c = 20.3 ± 0.3°C and P_m = 203.8 ± 2.1 kPa, differences of 1.5 and 1.0 percent, respectively.

Furthermore, the sensors used to monitor these parameters are subject to design errors. According to the manufacturer's specifications, the error in K-type thermocouples is ± 5°C while the E-type thermocouples are subject to an error of ± 2°C. The Omega pressure transducer has an error of ± 0.5 percent, based on manufacturer's data.

b. Determining the Resonance Frequency

Prior to onset, the fitting function used to determine the resonance frequency, f_o is accurate to approximately 0.1 percent. Above onset, f_o is determined by analyzing the DFT of the sampled waveform. A sampling rate of 5 μsec for a 4000 point record corresponds to a frequency range of 2000 Hz. This results in an accuracy of 0.5 Hz per point or 0.3 percent for f_o = 160 Hz. A larger error in the frequency occurs as a result of calculating f_o. It was stated in Chapter II that the computation neglects dispersion due to attenuation. The result is that the theory slightly overpredicts f_o. However, the maximum error is approximately 2 percent.

3. Steady State

Figures 17 through 20 show the waveform and DFT of data collected after the prime mover had reached steady state above onset at approximately 80 kPa. Figs. 17 and 18

correspond to a ΔT_m of 382.8 °C, while Figs 19 and 20 correspond to a ΔT_m of 419.8°C. An extensive set of data is presented in the Appendix. It is seen from these figures that the waveforms become highly nonlinear at higher temperature differences. These results are consistent with Lin's data obtained in helium. A future goal of this research is to predict these waveforms.

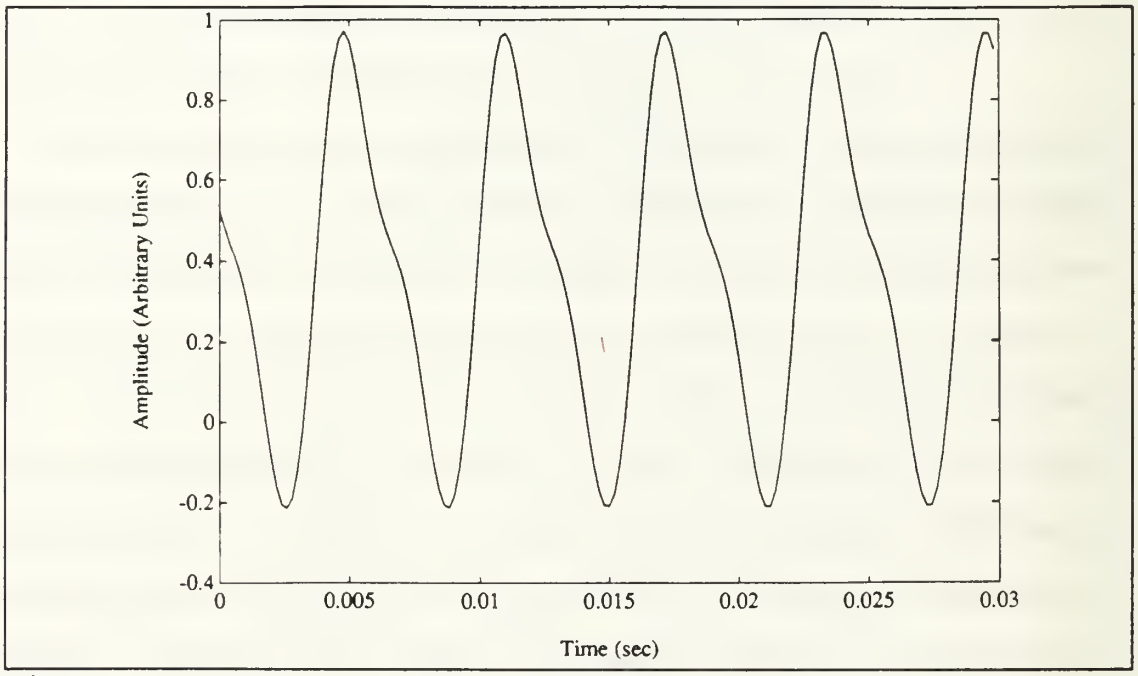

Figure 17. Plot of waveform obtained at steady state. P = 80.1 kPa. ΔT_m = 382.8 °C.

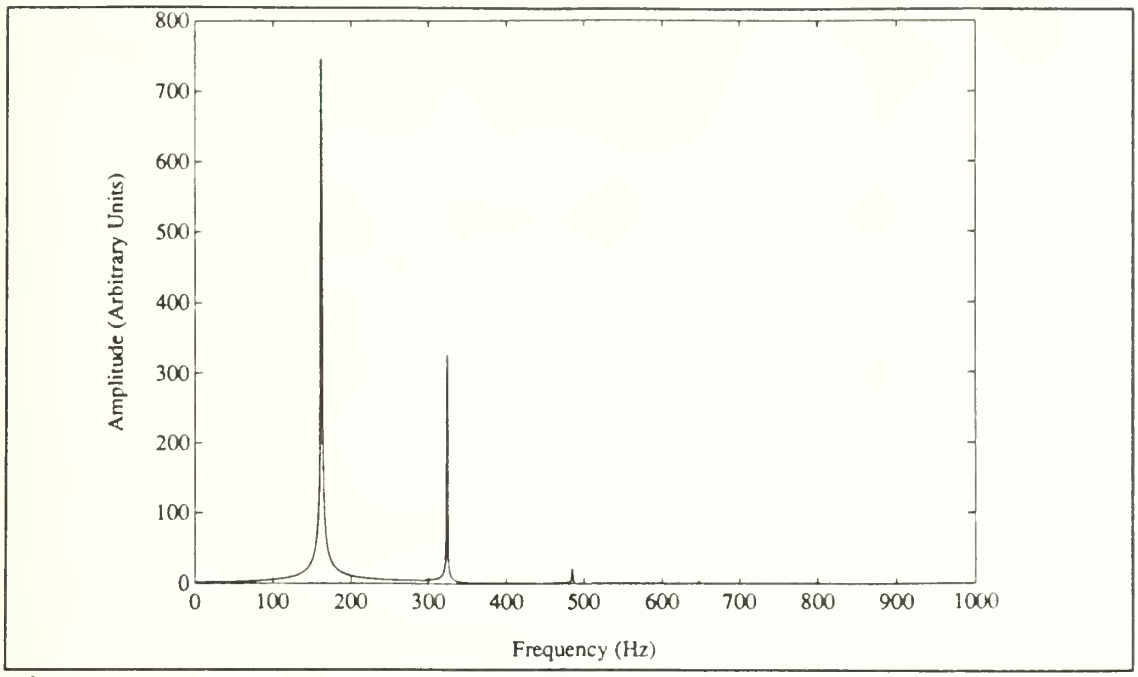

Figure 18. Plot of DFT of data obtained at steady state. P = 80.1 kPa. ΔT_m = 382.8 °C.

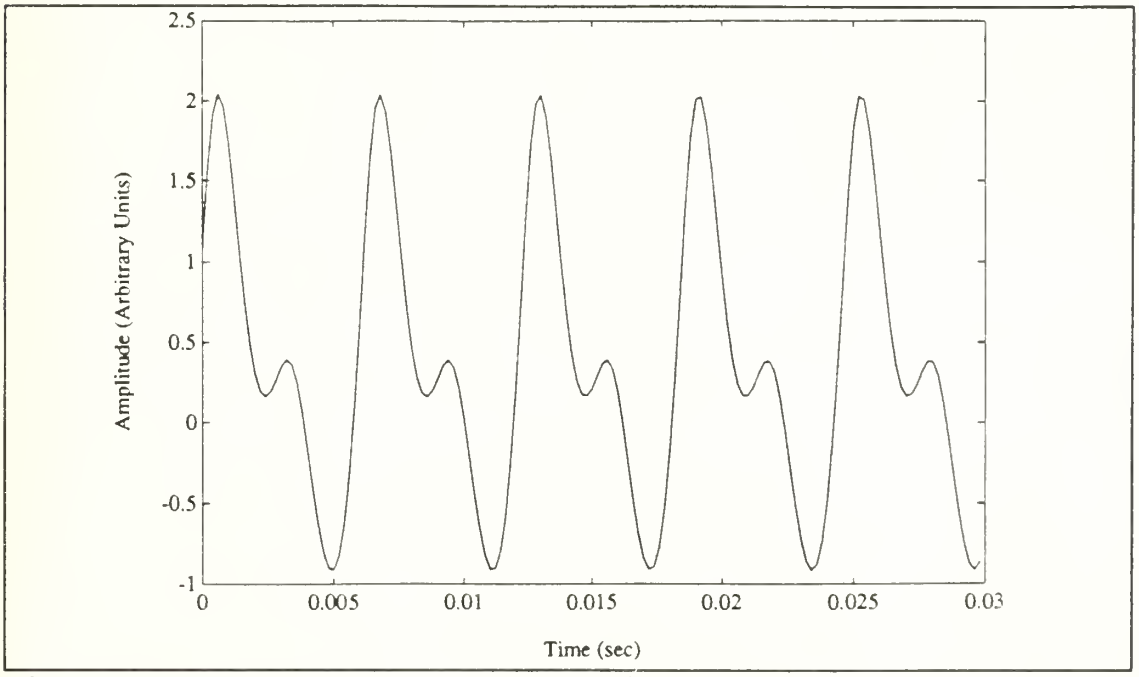

Figure 19. Plot of waveform obtained at steady state. P = 80.3 kPa. ΔT_m = 419.8 °C.

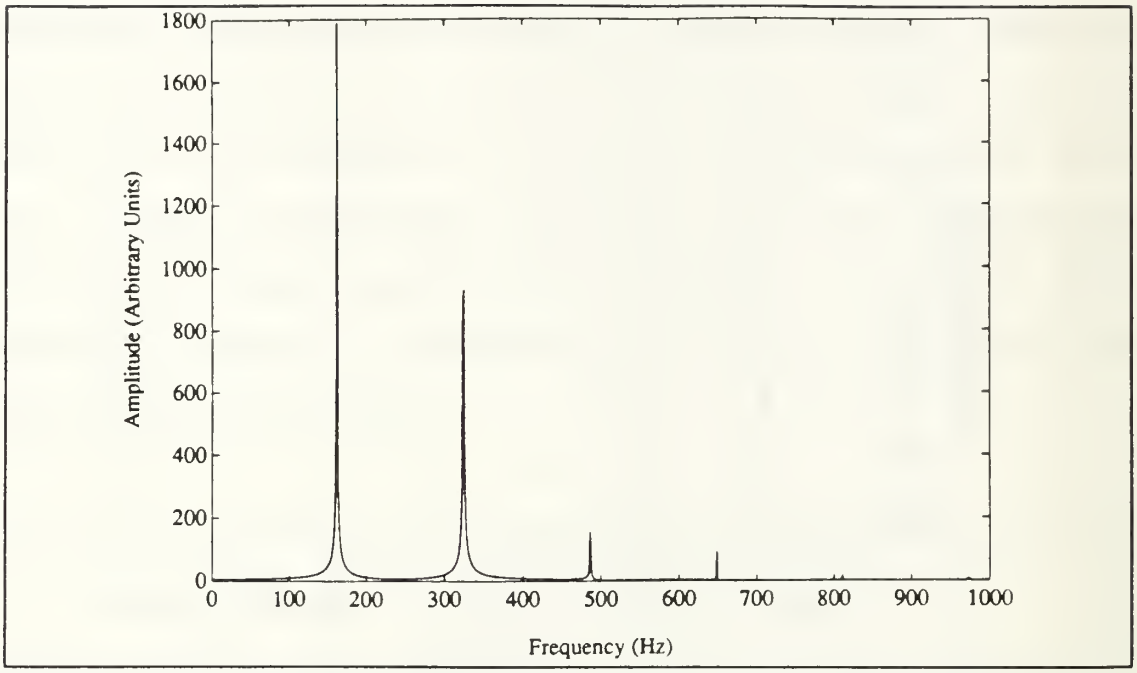

Figure 20. Plot of DFT of data obtained at steady state. P = 80.3 kPa. ∇T_m = 419.8 °C.

V. CONCLUSIONS

The purpose of this thesis was to investigate the behavior of an argon-filled thermoacoustic prime mover. The reasons for this investigation were two-fold. First, the data collected below and immediately above thermoacoustic onset allowed a verification of theoretical predictions begun in previous research. Since the previous work used helium as the working fluid, this experiment varied the input parameters by using argon, instead. Additionally, this data is the first to span onset. Our results indicate that the theory provides a good agreement with measurement, although some discrepancies do exist. At lower mean gas pressures, the prime mover's behavior begins to deviate from theory at higher values of ΔT_m. This deviation may be due to imperfections in the prime mover stack geometry. There is also a tendency to underpredict the attenuation.

Data was also obtained at steady state. These data show that the waveforms are highly nonlinear. One of the ultimate goals of our research is to be able to predict the shape of these waveforms. At this time we are working with a model that predicts the waveforms of high amplitude standing waves in simple tubes. The inputs to the model are the resonance frequency and the Q of the modes of the tube. Once a prime mover has gone into oscillation, it is no longer

possible to measure these parameters. We will have to rely on theoretical values.

The good agreement between the measured and predicted values of 1/Q indicate that we will be able to provide a reasonably good input for the model. This discussion leads to a somewhat subtle, but important, point. Below onset, Q is determined by fitting the measured frequency response to the ideal frequency response of a simple tube. The quality of the agreement indicates that, to a good approximation, the prime mover behaves like a simple tube having a uniform cross section and temperature distribution!

APPENDIX

PLOTS OF STEADY STATE DATA

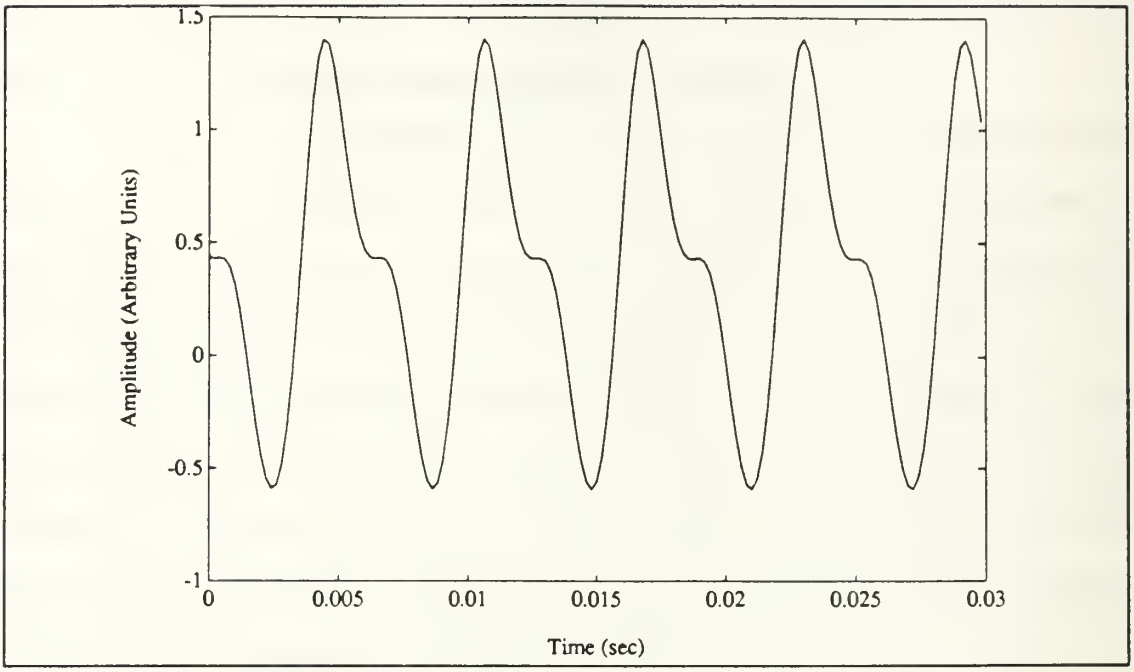

Figure 21. Plot of waveform obtained at steady state. P = 81.1 kPa. ΔT_m = 398.3 °C.

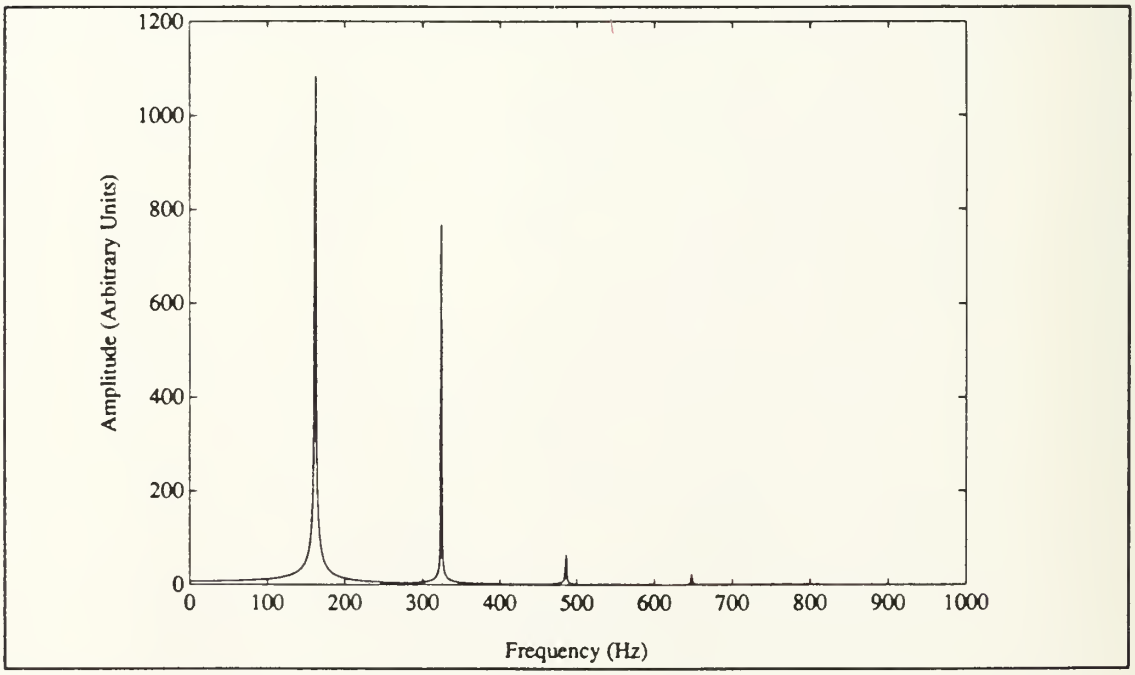

Figure 22. Plot of DFT of data obtained at steady state. P = 81.1 kPa. ΔT_m = 398.3 °C.

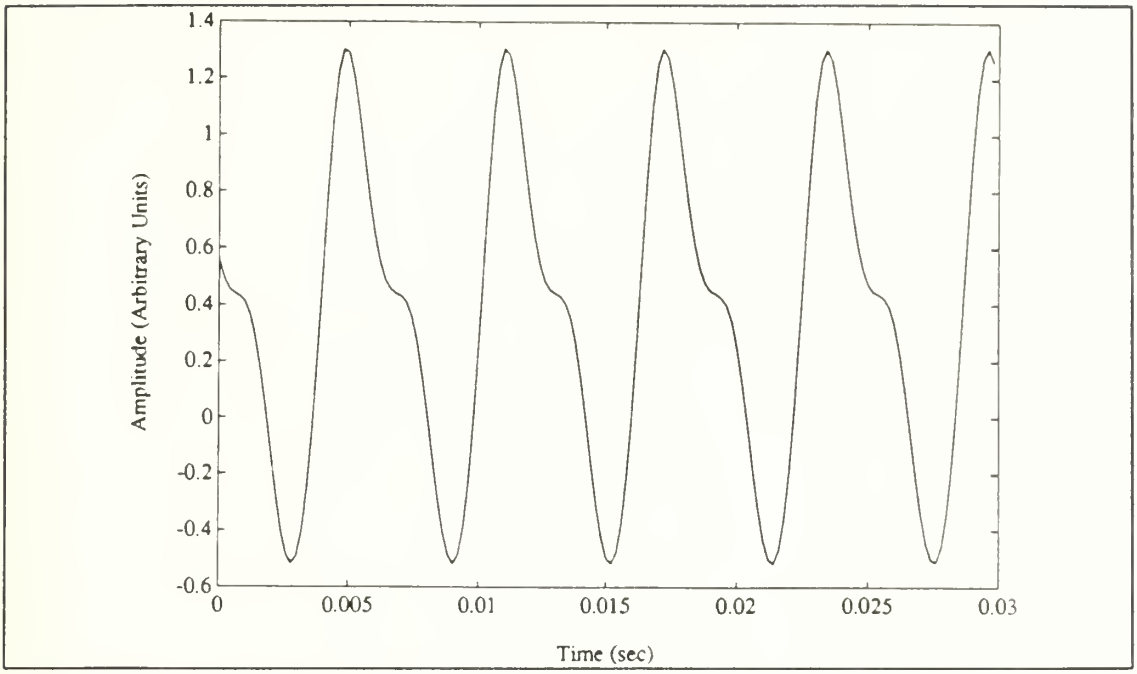

Figure 23. Plot of waveform obtained at steady state. P = 81.2 kPa. ΔT_m = 394.2 °C.

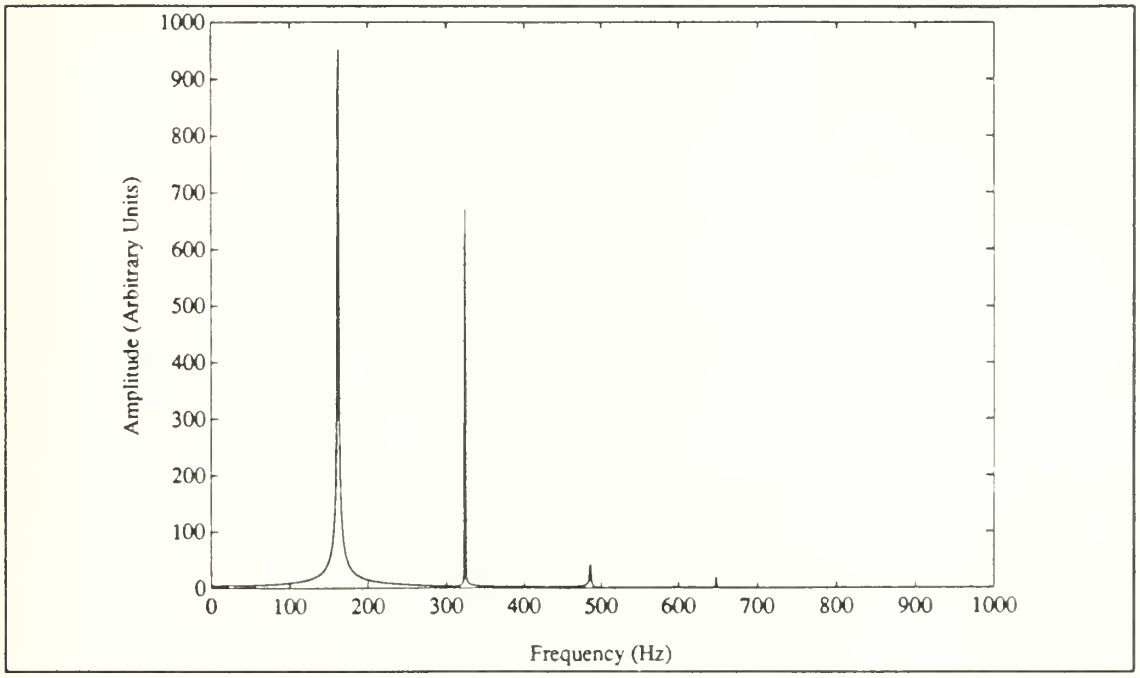

Figure 24. Plot of DFT of data obtained at steady state. P = 81.2 kPa. ΔT_m = 394.2 °C.

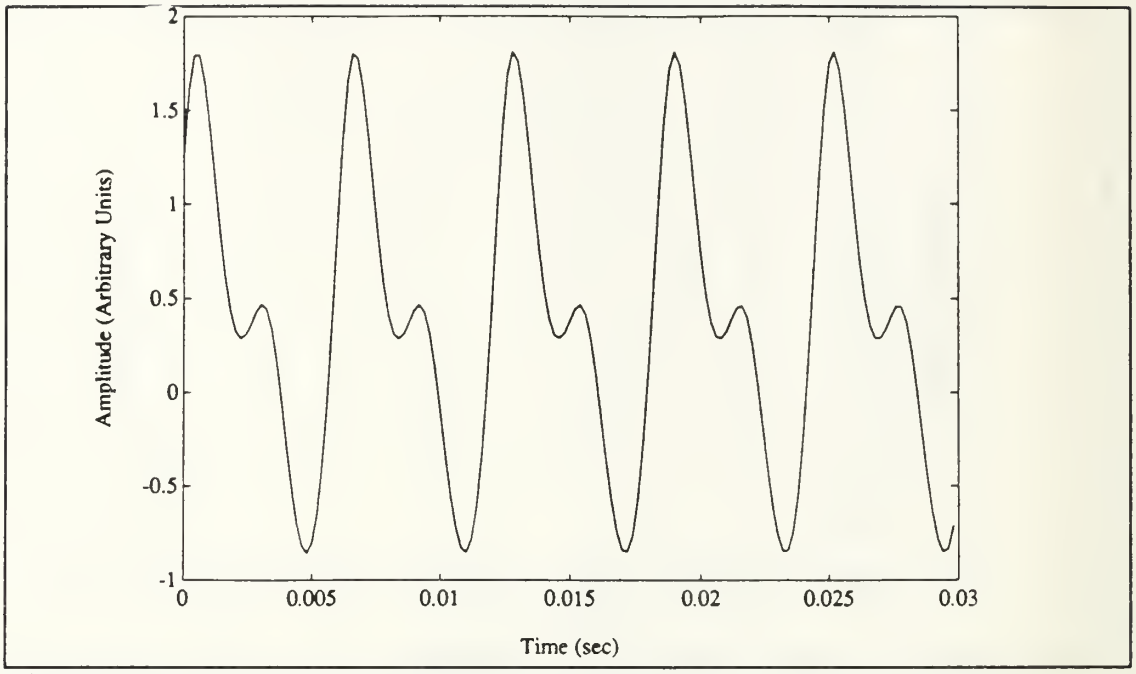

Figure 25. Plot of waveform obtained at steady state. P = 80.3 kPa. ΔT_m = 411.4 °C.

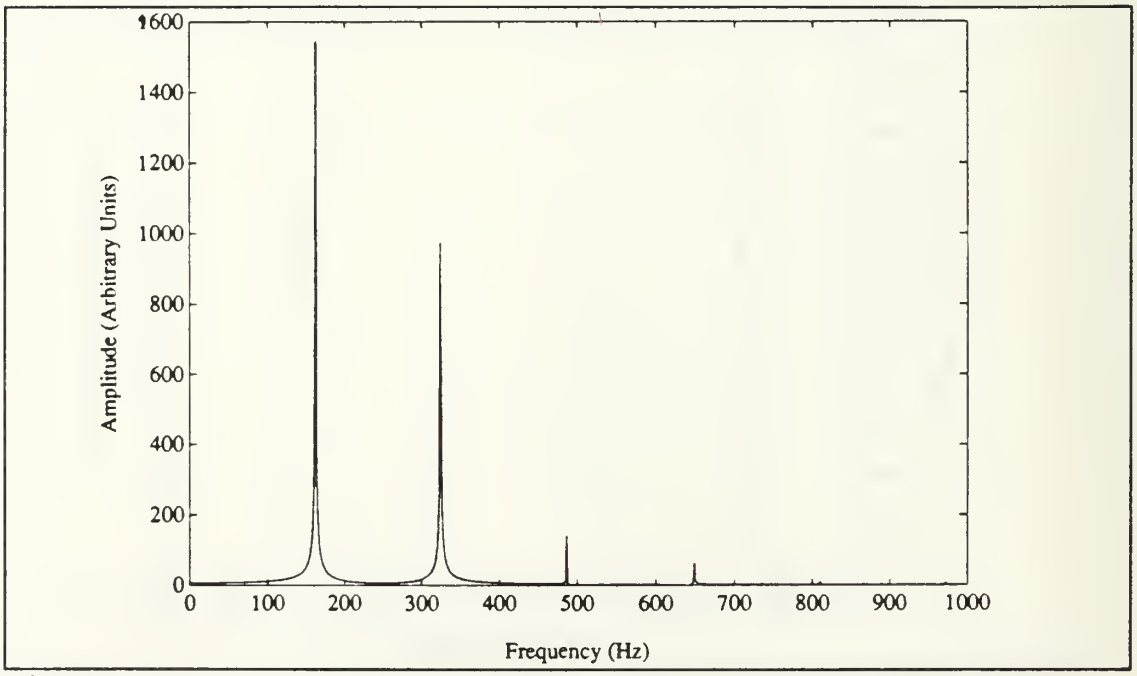

Figure 26. Plot of waveform obtained at steady state. P = 80.3 kPa. ΔT_m = 411.4 °C.

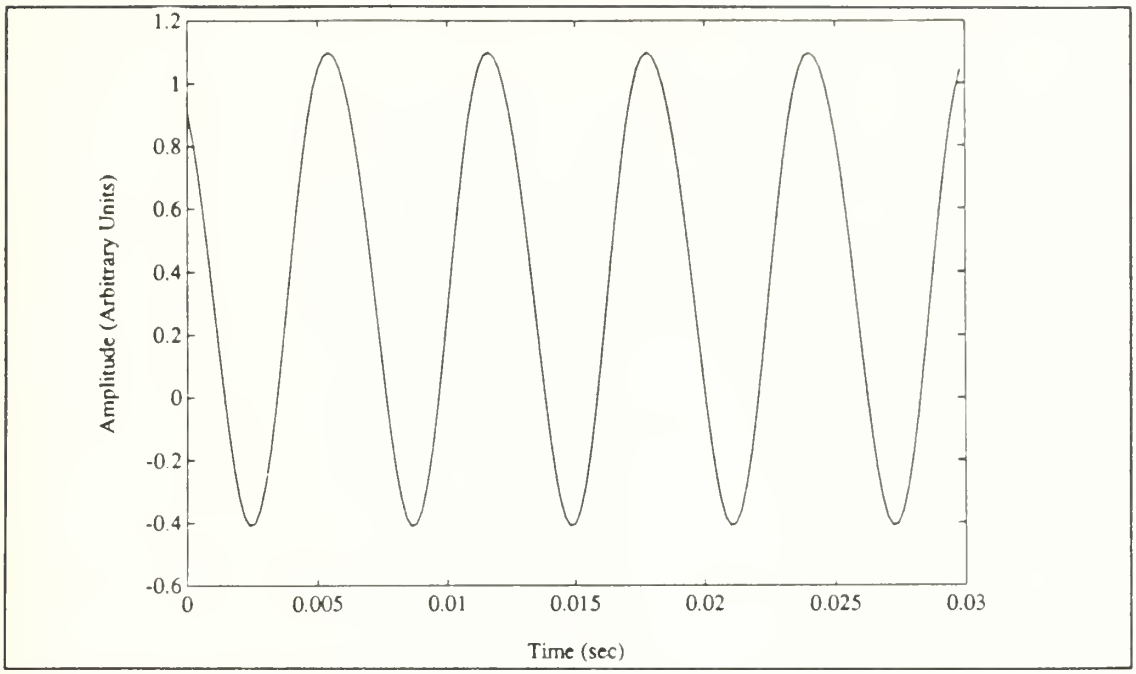

Figure 27. Plot of waveform obtained at steady state. P = 206.7 kPa. ΔT_m = 384.7 °C.

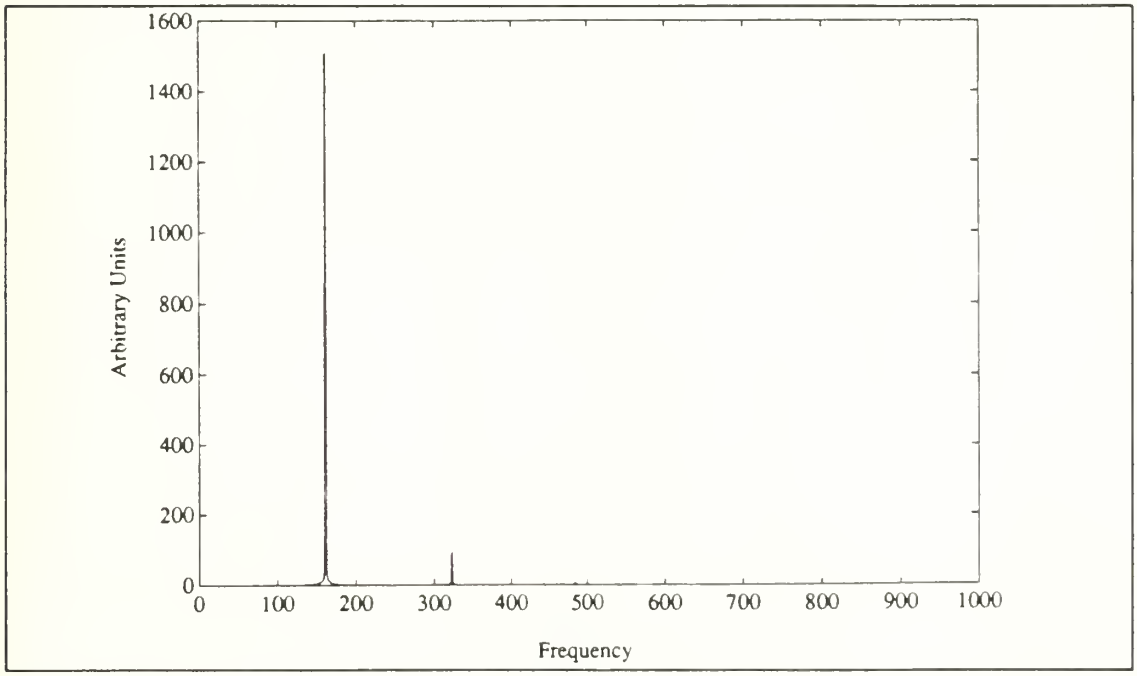

Figure 28. Plot of DFT of data obtained at steady state. P = 206.7 kPa. ΔT_m = 384.7 °C.

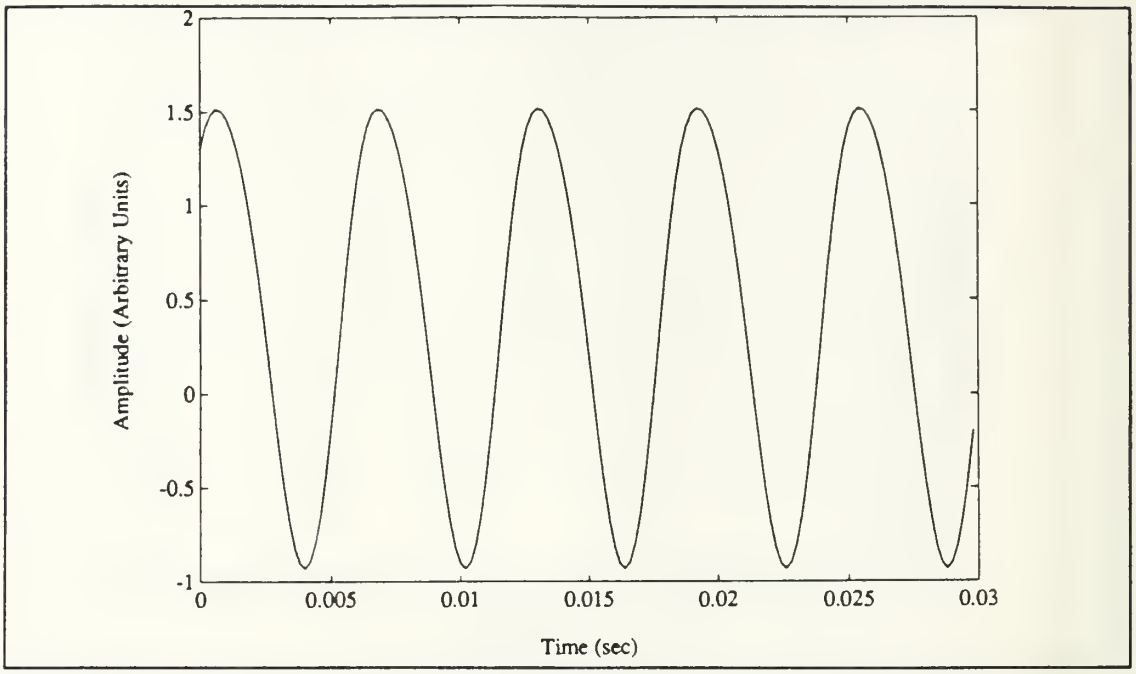

Figure 29. Plot of waveform obtained at steady state. P = 206.5 kPa. ΔT_m = 395.1 °C.

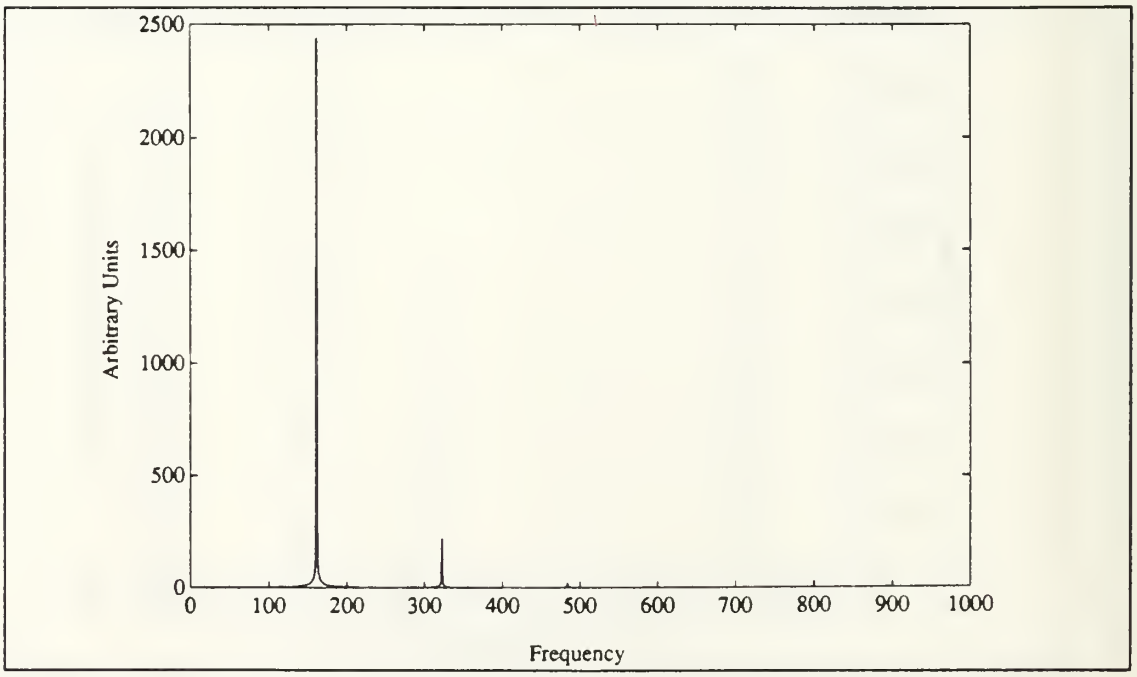

Figure 30. Plot of DFT of data obtained at steady state. P = 206.5 kPa. ΔT_m = 395.1 °C.

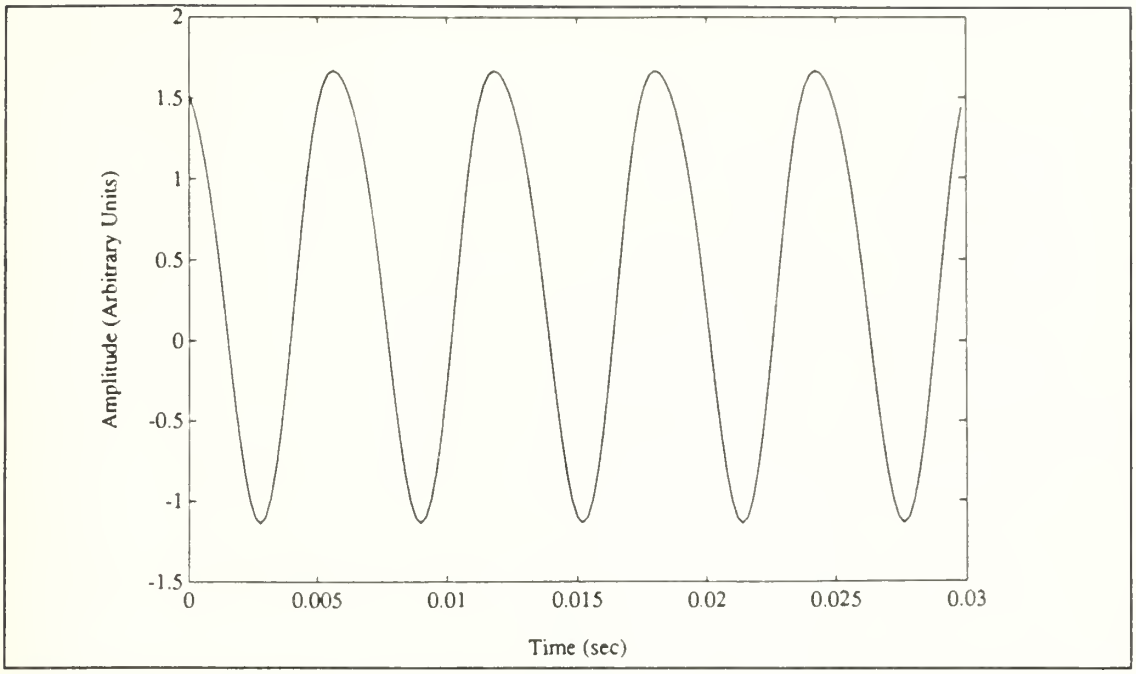

Figure 31. Plot of waveform obtained at steady state. P = 206.7 kPa. ΔT_m = 398.7 °C.

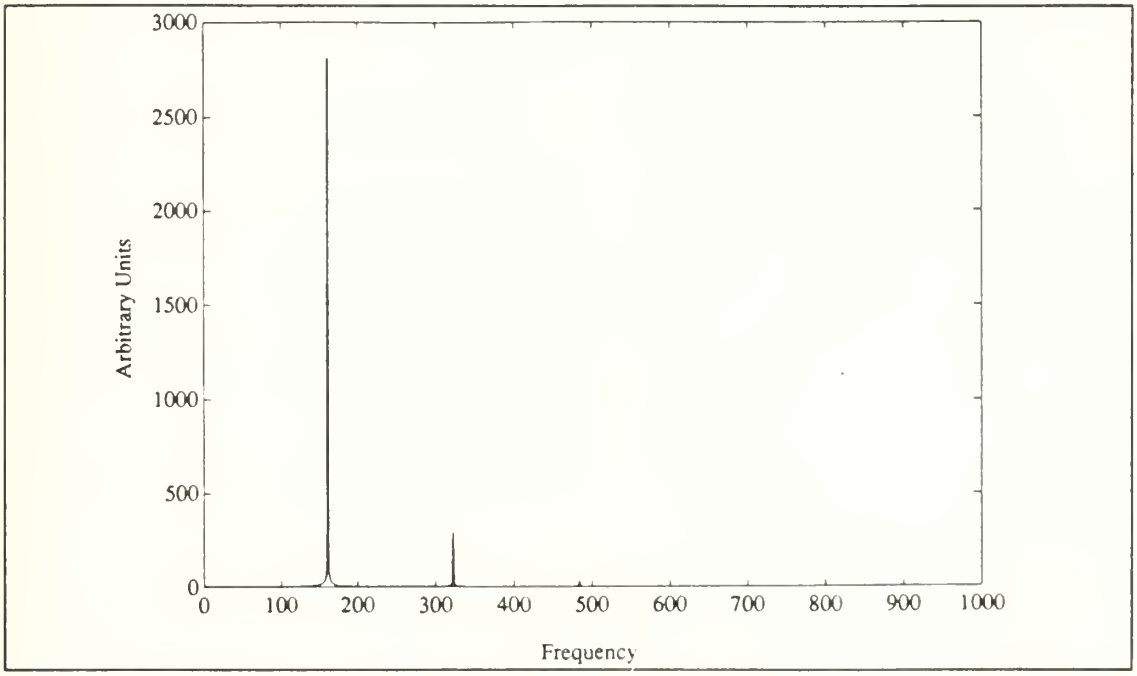

Figure 32. Plot of DFT of data obtained at steady state. P = 206.7 kPa. ΔT_m = 398.7 °C.

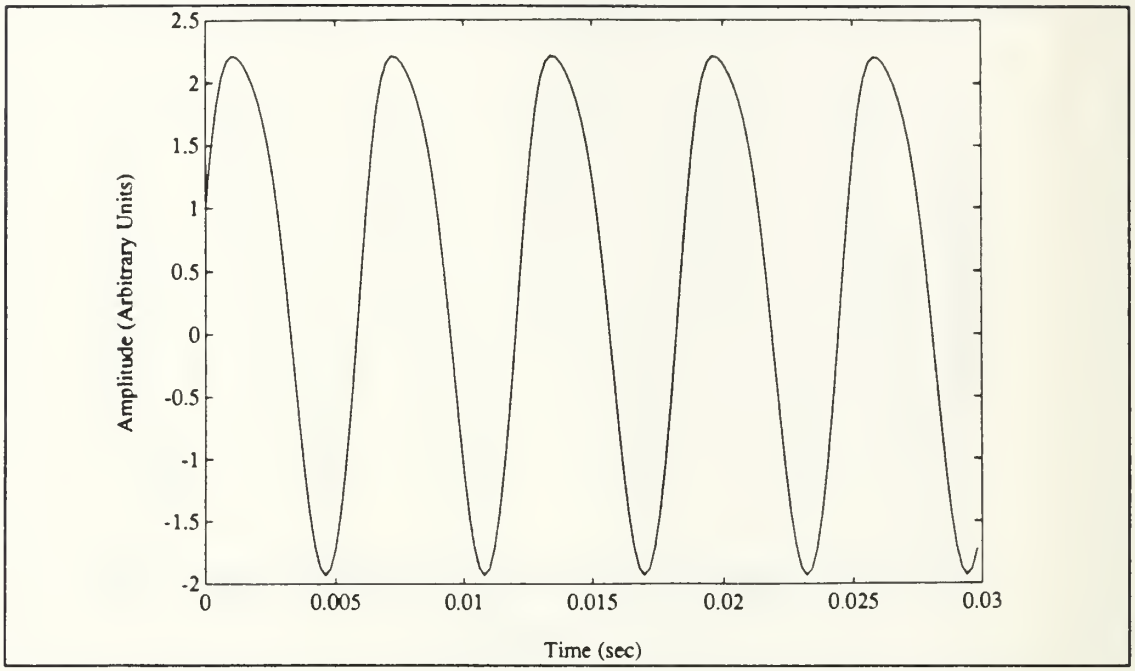

Figure 33. Plot of waveform obtained at steady state. P = 204.8 kPa. ΔT_m = 411.5 °C.

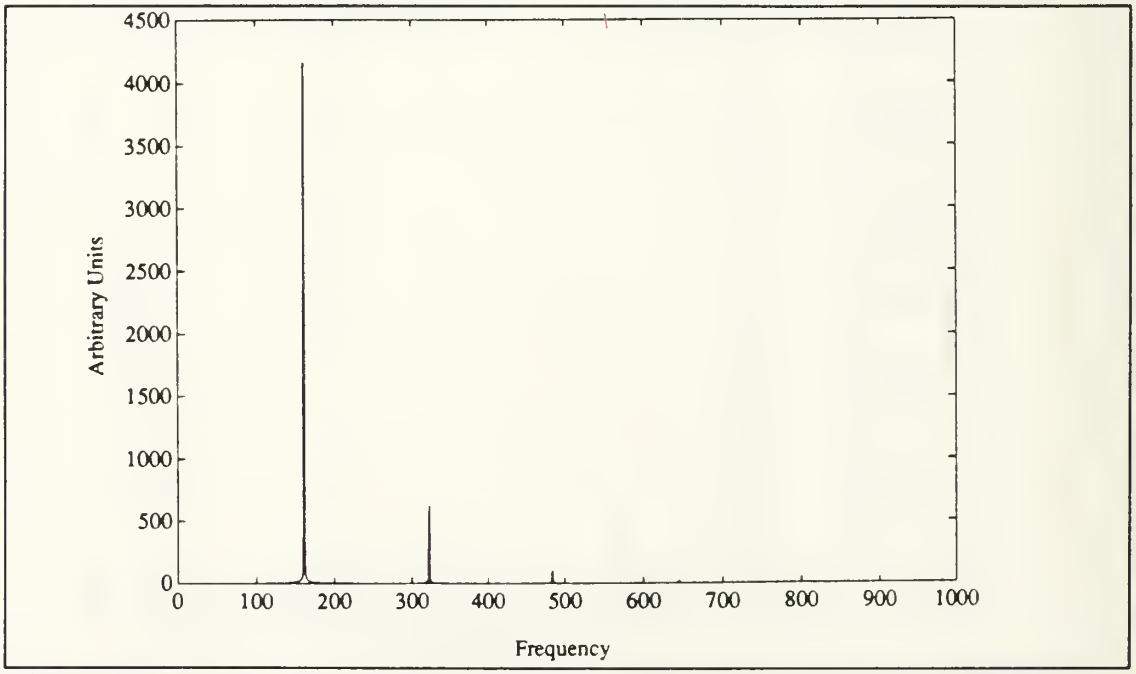

Figure 34. Plot of DFT of data obtained at steady state. P = 204.8 kPa. ΔT_m = 411.5 °C.

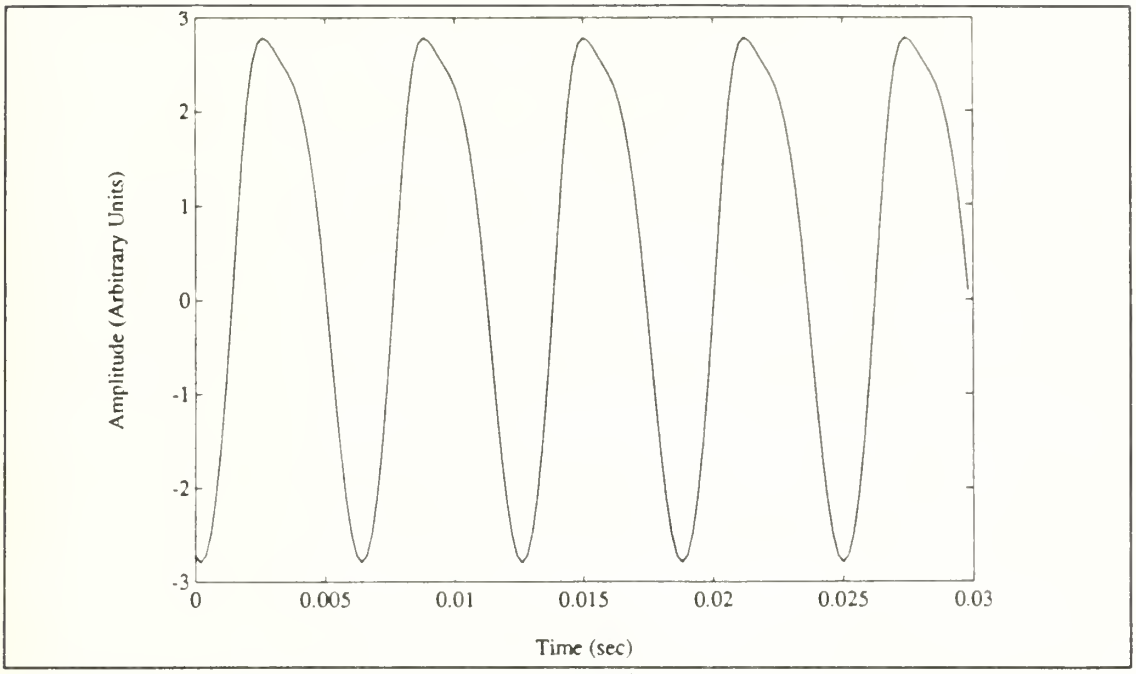

Figure 35. Plot of waveform obtained at steady state. P = 207.7 kPa. ΔT_m = 416.5 °C.

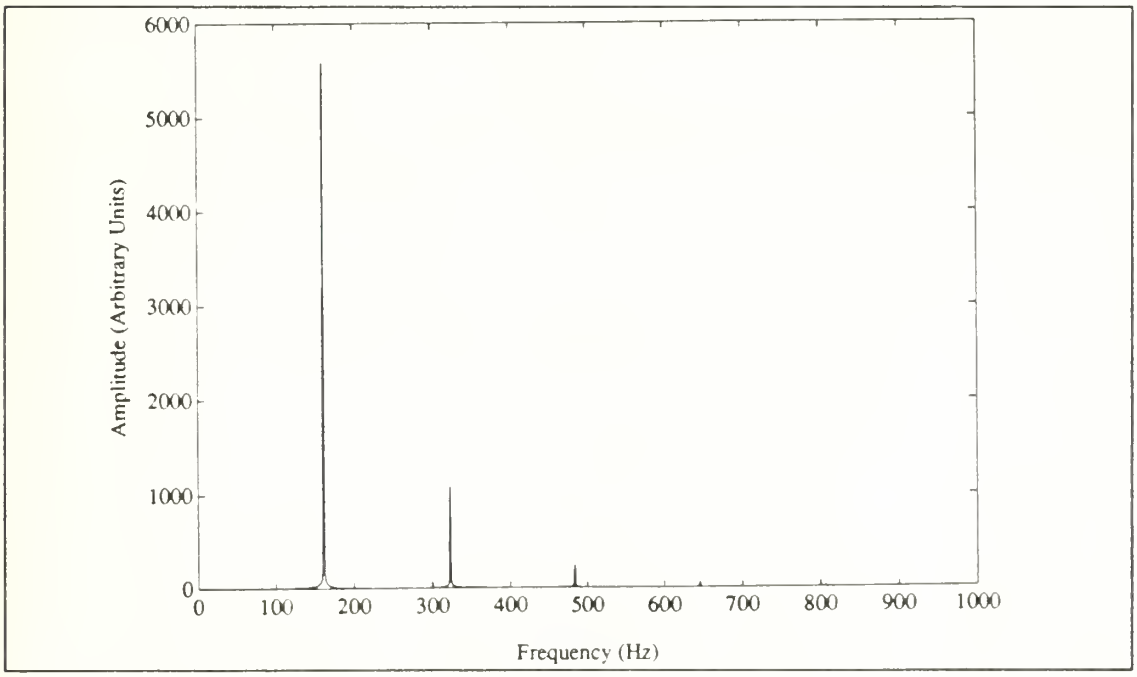

Figure 36. Plot of DFT of data obtained at steady state. P = 207.7 kPa. ΔT_m = 416.5 °C.

LIST OF REFERENCES

Atchley, Anthoney A., Unpublished Research, Naval Postgraduate School, Monterey, California, December 1991.

Bowers, Earl C., Investigation of a Heat Driven Thermoacoustic Prime Mover Above Onset of Self-Oscillation, Master's Thesis, Naval Postgraduate School, Monterey, California, October 1991.

Chen, Chih-Lyeu, Experimental Investigation of Energy Dissipation in Finite Amplitude Standing Waves, Master's Thesis, Naval Postgraduate School, Monterey, California, June 1989.

Lin, Hsio-Tseng, Investigation of a Heat Driven Thermoacoustic Prime Mover, Master's Thesis, Naval Postgraduate School, Monterey, California, December 1989.

Strum, Robert D., and Kirk, Donald E., First Principles of Dicrete Systems and Digital Signal Processing, Addison-Wesley, 1988.

Swift, G. W., "Thermoacoustic Engines," J. Acoust. Soc. Am. Vol. 84, October 1988.

INITIAL DISTRIBUTION LIST

1.	Defense Technical Information Center Cameron Station Alexandria, Virginia 22304-6145	2
2.	Library, Code 0142 Naval Postgraduate School Monterey, California 93943-5002	2
3.	Prof. Anthony A. Atchley, Code PH/Ay Physics Department Naval Postgraduate School Monterey, California 93943-5002	5
4.	Dr. D. Felipe Gaitan, Code PH Physics Department Naval Postgraduate School Monterey, California 93943-5002	1
5.	Dr. Logan E. Hargrove Office of Naval Research Physics Division - Code 1112 800 N. Quincy Street Arlington, Virginia 22217-5000	1
6.	Dr. Henry E. Bass Physical Acoustics Research Laboratory University of Missippi University, Missippi 38677	1
7.	LT. J. Dietrick Lamade II 410 School Street Marshfield, Massachusetts 02050	2